

THIS IS A PREPRINT --- SUBJECT TO CORRECTION

Decline Curve Analysis Using Type Curves

By

M. J. Fetkovich, Member AIME, Phillips Petroleum Co.

© Copyright 1973

American Institute of Mining, Metallurgical, and Petroleum Engineers, Inc.

This paper was prepared for the 48th Annual Fall Meeting of the Society of Petroleum Engineers of AIME, to be held in Las Vegas, Nev., Sept. 30-Oct. 3, 1973. Permission to copy is restricted to an abstract of not more than 300 words. Illustrations may not be copied. The abstract should contain conspicuous acknowledgment of where and by whom the paper is presented. Publication elsewhere after publication in the JOURNAL OF PETROLEUM TECHNOLOGY or the SOCIETY OF PETROLEUM ENGINEERS JOURNAL is usually granted upon request to the Editor of the appropriate journal provided agreement to give proper credit is made.

Discussion of this paper is invited. Three copies of any discussion should be sent to the Society of Petroleum Engineers office. Such discussion may be presented at the above meeting and, with the paper, may be considered for publication in one of the two SPE magazines.

ABSTRACT

This paper shows that the decline-curve analysis approach does have a solid fundamental basis. The exponential decline is shown to be a longtime solution of the constant-pressure case. The constant-pressure infinite and finite reservoir solutions are placed on a common dimensionless curve with all the standard "empirical" exponential, hyperbolic, and harmonic decline-curve equations. Simple combinations of material balance equations and new forms of oil well rate equations for solution-gas drive reservoirs illustrate under what circumstances specific values of the hyperbolic decline exponent ($1/b$) or " b " should result.

Log-log type curve analysis can be performed on declining rate data (constant-terminal pressure case) completely analogous to the log-log type curve matching procedure presently being employed with constant-rate case pressure transient data. Production forecasting is done by extending a line drawn through the rate-time data overlain along the uniquely matched or best theoretical type curve. Future rates are then simply read from the real time scale on which the rate-time data is plotted. The ability to calculate kh from decline-curve data by type

References and illustrations at end of paper.

curve matching is demonstrated.

This paper demonstrates that decline-curve analysis not only has a solid fundamental base, but provides a tool with more diagnostic power than has previously been suspected. The type curve approach provides unique solutions upon which engineers can agree, or shows when a unique solution is not possible with a type curve only.

INTRODUCTION

Rate-time decline-curve extrapolation is one of the oldest and most often used tools of the petroleum engineer. The various methods used have always been regarded as strictly empirical and not very scientific. Results obtained for a well or lease are subject to a wide range of alternate interpretations, mostly as a function of the experience and objectives of the evaluator. Recent efforts in the area of decline-curve analysis have been directed towards a purely computerized statistical approach. Its basic objective being to arrive at a unique "unbiased" interpretation. As pointed out in a comprehensive review of the literature by Ramsay¹, "in the period from 1964 to date, (1968), several additional papers were published which contribute to the understanding of decline-curves but add little new

technology".

A new direction for decline-curve analysis was given by Slider² with his development of an overlay method to analyze rate-time data. Because his method was rapid and easily applied, it was used extensively by Ramsay in his evaluation of some 200 wells to determine the distribution of the decline-curve exponent term "b". Gentry's³ Fig. 1 displaying the Arps'⁴ exponential, hyperbolic, and harmonic solutions all on one curve could also be used as an overlay to match all of a wells' decline data. He did not, however, illustrate this in his example application of the curve.

The overlay method of Slider is similar in principal to the log-log type curve matching procedure presently being employed to analyze constant-rate pressure build-up and drawdown data⁵⁻⁹. The exponential decline, often used in decline-curve analysis, can be readily shown to be a long-time solution of the constant-pressure case¹⁰⁻¹³. It followed then that a log-log type curve matching procedure could be developed to analyze decline-curve data.

This paper demonstrates that both the analytical constant-pressure infinite (early transient period for finite systems) and finite reservoir solutions can be placed on a common dimensionless log-log type curve with all the standard "empirical" exponential, hyperbolic, and harmonic decline curve equations developed by Arps. Simple combinations of material balance equations and new forms of oil well rate equations from the recent work of Fetkovich¹⁴ illustrate under what circumstances specific values of the hyperbolic decline exponent "b" should result in dissolved-gas drive reservoirs. Log-log type curve analysis is then performed using these curves with declining rate data completely analogous to the log-log type curve matching procedure presently being employed with constant-rate case pressure transient data.

BASIC EQUATIONS

ARPS' RATE-TIME EQUATIONS

Nearly all conventional decline-curve analysis is based on the empirical rate-time equations given by Arps⁴ as

$$\frac{q(t)}{q_i} = \frac{1}{[1+bd_i t]^{\frac{1}{b}}} \dots (1)$$

For b = 0, we can obtain the exponential decline equation from Eq. 1

$$\frac{q(t)}{q_i} = \frac{1}{D_i t} \dots (2)$$

and for b = 1, referred to as harmonic decline, we have

$$\frac{q(t)}{q_i} = \frac{1}{[1+D_i t]} \dots (3)$$

A unit solution (D_i = 1) of Eq. 1 was developed for values of "b" between 0 and 1 in 0.1 increments. The results are plotted as a set of log-log type curves (Fig. 1) in terms of a decline-curve dimensionless rate

$$q_{Dd} = \frac{q(t)}{q_i} \dots (4)$$

and a decline-curve dimensionless time

$$t_{Dd} = D_i t \dots (5)$$

From Fig. 1 we see that when all the basic decline-curves and normal ranges of "b" are displayed on a single graph, all curves coincide and become indistinguishable at t_{Dd} ≈ 0.3. Any data existing prior to a t_{Dd} of 0.3 will appear to be an exponential decline regardless of the true value of b and thus plot as a straight line on semi-log paper. A statistical or least-squares approach could calculate any value of b between 0 and 1.

ANALYTICAL SOLUTIONS (CONSTANT-PRESSURE AT INNER BOUNDARY)

Constant well pressure solutions to predict declining production rates with time were first published in 1933 by Moore, Schilthuis and Hurst¹⁰, and Hurst¹¹. Results were presented for infinite and finite, slightly compressible, single-phase plane radial flow systems. The results were presented in graphical form in terms of a dimensionless flow rate and a dimensionless time. The dimensionless flow rate q_D can be expressed as

$$q_D = \frac{141.3 q(t) \mu B}{kh(p_i - p_{wf})} \dots (6)$$

and the dimensionless time t_D as

$$t_D = \frac{0.00634 kt}{\phi \mu_c r_w^2} \dots (7)$$

The original publications did not include tabular values of q_D and t_D. For use in this paper infinite solution values were obtained from Ref. 15, while the finite values were obtained from Ref. 16. The infinite solution, and finite solutions for r_e/r_w from 10 to 100,000, are plotted on Figs. W2-a and 2-b.

Most engineers utilize the constant-pressure solution not in a single constant-pressure problem but as a series of constant-pressure step functions to solve water influx problems using the dimensionless cumulative production Q_D (13). The relationship between Q_D and q_D is

$$\frac{d(Q_D)}{dt_D} = q_D \dots (8)$$

Fetkovich¹⁷ presented a simplified approach to water influx calculations for finite systems that gave results which compared favorably with the more rigorous analytical constant-pressure solutions. Equation 3 of his paper, for a constant-pressure p_{wf} , can be written as

$$q(t) = \frac{J_o (p_i - p_{wf})}{e^{\left[\frac{(q_i)_{max}}{N_{pi}} \right] t}} \dots (9)$$

but

$$q_i = J_o (p_i - p_{wf}) \dots (10)$$

and

$$J_o = \frac{(q_i)_{max}}{F_i} \dots (11)$$

Substituting Eq. 11 into 10 we can write

$$(q_i)_{max} = \frac{q_i}{\left[1 - \frac{p_{wf}}{p_i} \right]} \dots (12)$$

Now substituting Eq. 10 and 12 into 9 we obtain

$$\frac{q(t)}{q_i} = e^{-\left[\frac{q_i t}{\left(1 - \frac{p_{wf}}{p_i} \right) N_{pi}} \right]} \dots (13)$$

Equation 13 can be considered as a derivation of the exponential decline equation in terms of reservoir variables and the constant-pressure imposed on the well. For the same well, different values of a single constant back-pressure p_{wf} will always result in an exponential decline i.e., the level of back-pressure does not change the type of decline. For $p_{wf} = 0$, a more realistic assumption for a well on true wide-open decline, we have

$$\frac{q(t)}{q_i} = e^{-\left[\frac{(q_i)_{max}}{N_{pi}} \right] t} \dots (14)$$

In terms of the empirical exponential decline-curve, Eq. 2, D_i is then defined as

$$D_i = \frac{(q_i)_{max}}{N_{pi}} \dots (15)$$

In terms of a dimensionless time for decline-curve analysis we have from Eqs. 5 and 15

$$t_{Dd} = \left[\frac{(q_i)_{max}}{N_{pi}} \right] t \dots (16)$$

Defining N_{pi} and $(q_i)_{max}$ in terms of reservoir variables,

$$N_{pi} = \frac{\pi (r_e^2 - r_w^2) \phi c_t h p_i}{5.615 B} \dots (17)$$

and

$$(q_i)_{max} = \frac{khp_i}{141.3 \mu B \left[\ln \left(\frac{r_e}{r_w} \right) - \frac{1}{2} \right]} \dots (18)$$

The decline-curve dimensionless time, in terms of reservoir variables, becomes

$$t_{Dd} = \frac{0.00634 kt}{\phi \mu c_t r_w^2} \cdot \frac{1}{\frac{1}{2} \left[\left(\frac{r_e}{r_w} \right)^2 - 1 \right] \left[\ln \left(\frac{r_e}{r_w} \right) - \frac{1}{2} \right]} \dots (19)$$

or

$$t_{Dd} = \frac{t_D}{\frac{1}{2} \left[\left(\frac{r_e}{r_w} \right)^2 - 1 \right] \left[\ln \left(\frac{r_e}{r_w} \right) - \frac{1}{2} \right]} \dots (20)$$

To obtain a decline-curve dimensionless rate q_{Dd} in terms of q_D

$$q_{Dd} = \frac{q(t)}{q_i} = q_D \left[\ln \left(\frac{r_e}{r_w} \right) - \frac{1}{2} \right] \dots (21)$$

or

$$q_{Dd} = \frac{q(t)}{\frac{kh (p_i - p_{wf})}{141.3 \mu B \left[\ln \left(\frac{r_e}{r_w} \right) - \frac{1}{2} \right]}} \dots (22)$$

The published values of q_D and t_D for the infinite and finite constant-pressure solutions were thus transformed into a decline-curve dimensionless rate and time, q_{Dd} and t_{Dd} , using Eqs. 20 and 21. Fig. 3 is a plot of the newly defined dimensionless rate and time, q_{Dd} and t_{Dd} , for various values of r_e/r_w .

At the onset of depletion, (a type of pseudo-steady state) all solutions for various values of r_e/r_w develop exponential decline and converge to a single curve. Figure 4 is a combination of the constant-pressure analytical solutions and the standard "empirical" exponential, hyperbolic, and harmonic decline-curve solutions on a single dimensionless curve. The exponential decline is common to both the analytical and empirical solutions. Note from the composite curve that rate data existing only in the transient period of the constant terminal pressure solution, if analyzed by the empirical Arps approach, would require values of "b" much greater than 1 to fit the data.

SOLUTIONS FROM RATE AND MATERIAL BALANCE EQUATIONS

The method of combining a rate equation and material balance equation for finite systems to obtain a rate-time equation was outlined in Ref. 17. The rate-time equation obtained using this simple approach, which neglects early transient effects, yielded surprisingly good results when compared to those obtained using more rigorous analytical solutions for finite aquifer systems. This rate-equation material-balance approach was used to derive some useful and instructive decline-curve equations for solution-gas drive reservoirs and gas reservoirs.

RATE EQUATIONS

Until recently, no simple form of a rate equation existed for solution-gas drive reservoir shut-in pressure. Fetkovich¹⁴ has proposed a simple empirical rate equation for solution-gas drive reservoirs that yields results which compare favorably with computer results obtained using two-phase flow theory. The proposed rate equation was given as

$$q_o = J'_{oi} \left(\frac{\bar{p}_R}{\bar{p}_{Ri}} \right) (\bar{p}_R^2 - p_{wf}^2)^n \dots (23)$$

where n will be assumed to lie between 0.5 and 1.0.

Although the above equation has not been verified by field results, it offers the opportunity to define the decline exponent

(1/b) in terms of the back pressure curve slope (n) and to study its range of expected values. Also, the initial decline rate D_i can be expressed in terms of reservoir variables. One further simplification used in the derivations is that $p_{wf} = 0$. For a well on decline, p_{wf} will usually be maintained at or near zero to maintain maximum flow rates. Equation 23 then becomes

$$q_o = J'_{oi} \left(\frac{\bar{p}_R}{\bar{p}_{Ri}} \right) (\bar{p}_R^{2n}) \dots (23A)$$

The form of Eqs. 23 and 23A could also be used to represent gas well behavior with a pressure dependent interwell permeability effect defined by the ratio (\bar{p}_R/\bar{p}_{Ri}) . The standard form of the gas well rate equation is usually given as

$$q_g = C_g (\bar{p}_R^2 - p_{wf}^2)^n \dots (24)$$

MATERIAL BALANCE EQUATIONS

Two basic forms of a material balance equation are investigated in this study, p_R is linear with N or G, and \bar{p}_R^2 is linear with N or G_p (See Figs. 5a and b). The linear^p \bar{p}_R relationship for oil is

$$\bar{p}_R = - \left(\frac{\bar{p}_{Ri}}{N_{pi}} \right) N_p + \bar{p}_{Ri} \dots (25)$$

and for gas

$$\bar{p}_R = - \left(\frac{\bar{p}_{Ri}}{G_p} \right) G_p + \bar{p}_{Ri} \dots (26)$$

Equation 25 is a good approximation for totally undersaturated oil reservoirs, or is simply assuming that during the decline period \bar{p}_R vs. N can be approximated by a straight line.^p For gas reservoirs, Eq. 26 is correct for the assumption of gas compressibility (Z) = 1.

In terms of \bar{p}_R^2 being linear with cumulative production, we would have

$$\bar{p}_R^2 = - \left(\frac{\bar{p}_{Ri}^2}{N_{pi}} \right) N_p + \bar{p}_{Ri}^2 \dots (27)$$

This form of equation results in the typical shape of the pressure (\bar{p}_R) vs. cumulative production (N_p) relationship of a solution-gas

drive reservoir as depicted in Fig. 5-b. Applications would be more appropriate in non-prorated fields, i.e., wells are produced wide-open and go on decline from initial production. This would more likely be the case for much of the decline-curve data analyzed by Cutler¹⁸ obtained in the early years of the oil industry before proration.

RATE-TIME EQUATIONS, OIL WELLS

Rate-time equations using various combinations of material balance and rate equations were derived as outlined in Appendix B of Ref. 17. Using Eq. 23A and Eq. 25 the resulting rate-time equation is

$$\frac{q_o(t)}{q_{oi}} = \frac{1}{\left[2n \left(\frac{q_{oi}}{N_{pi}} \right) t + 1 \right]^{\frac{2n+1}{2n}}} \dots (28)$$

A unit solution, $(q_{oi}/N_{pi}) = 1$, of Eq. 28 is plotted as a log-log type curve for various values of n, Fig. 6, in terms of the decline-curve dimensionless time t_{Dd} . (For these derivations with $p_{wf} = 0$, $q_{oi} = (q_{oi})_{max}$. For the limiting range of back-pressure curve slopes (n) of 0.5 and 1.0, the Arps empirical decline-curve exponent (1/b) is 2.0 and 1.5 respectively or "b" = 0.500 and 0.667 respectively a surprisingly narrow range. To achieve an exponential decline, n must be equal to zero, and a harmonic decline requires $n \rightarrow \infty$. In practical applications, if we assume an n of 1.0 dominates in solution-gas (dissolved-gas) drive reservoirs and \bar{p}_R vs. N_p is linear for non-uniquely defined rate-time data, we would simply fit the rate-time data to the n = 1.0 curve. On the Arps' solution type curves, Fig. 1, we would use (1/b) = 2 or b = 0.667.

The rate-time equation obtained using Eq. 23A and Eq. 27 is

$$\frac{q_o(t)}{q_{oi}} = \frac{1}{\left[0.5 \left(\frac{q_{oi}}{N_{pi}} \right) t + 1 \right]^{2n+1}} \dots (29)$$

The unit solution of Eq. 29 is plotted as a log-log type curve for various values of n, Fig. 7. This solution results in a complete reversal from that of the previous one, n = 0 yields the harmonic decline and $n \rightarrow \infty$ gives the exponential decline. For the limiting range of back-pressure curve slopes (n) of 0.5 and 1.0, the decline-curve

exponent (1/b) is 2.0 and 3.0 or b = 0.500 and 0.333 respectively. This range of "b" values fits Arps' findings using Cutler's decline-curve data. He found that over 90 percent of the values of "b" lie in the range $0 \leq b \leq 0.5$. Ramsay¹ found a different distribution of the value of "b" analyzing modern rate decline data from some 202 leases. His distribution may be more a function of analyzing wells that have been subject to proration and are better represented by the assumptions underlying the rate-time solution given by Eq. 28, i.e., \bar{p}_R vs. N_p was linear over the decline period.

DECLINE-CURVE ANALYSIS OF GAS WELLS

Decline-curve analysis of rate-time data obtained from gas wells has been reported in only a few instances 19, 20. Using Eq. 24 with $p_{wf} = 0$, and Eq. 26, the rate-time equation for a gas well is

$$\frac{q_g(t)}{q_{gi}} = \frac{1}{\left[(2n-1) \left(\frac{q_{gi}}{G} \right) t + 1 \right]^{\frac{2n}{2n-1}}} \dots (30)$$

for all back-pressure curve slopes where $n > 0.5$.

For n = 0.5, the exponential decline is obtained

$$\frac{q_g(t)}{q_{gi}} = e^{-\left(\frac{q_{gi}}{G} \right) t} \dots (31)$$

The unit solutions of Eqs. 30 and 31 are plotted as a log-log type curve on Fig. 8. For the limiting range of back-pressure curve slopes (n) of 0.5 and 1.0, the Arps decline-curve exponent (1/b) is ∞ and 2, or b = 0 (exponential) and 0.500 respectively.

The effect of back-pressure on a gas well is demonstrated for a back-pressure curve slope n = 1.0 on Fig. 9. The back-pressure is expressed as a ratio of p_{wf}/p_i . Note that as $p_{wf} \rightarrow p_i$ ($\Delta p \rightarrow 0$) the type curve approaches exponential decline, the liquid case solution. Whereas back-pressure does not change the type of decline for the liquid-case solution it does change the type of decline in this case.

Using the more familiar rate and material balance equations for gas wells, we can obtain the cumulative-time relationship by integrating the rate-time equations 30 and 31 with

$$G_p = \int_0^t q_g(t) dt \dots (32)$$

For $n > 0.5$ we obtain

$$\frac{G_p}{G} = 1 - [1 + (2n-1) \left(\frac{q_{gi}}{G} \right) t]^{\frac{1}{(1-2n)}} \quad (33)$$

and $n = 0.5$

$$\frac{G_p}{G} = 1 - e^{-\left(\frac{q_{gi}}{G} \right) t} \quad (34)$$

Log-log type curves of Eqs. 33 and 34 could be prepared for convenience in obtaining cumulative production.

TYPE CURVE ANALYSIS

Recent papers by Agarwal, *et.al.*⁵, Ramey⁶, Raghavan, *et.al.*⁷ and Gringarten, *et.al.*⁸, have demonstrated or discussed the application and usefulness of a type-curve matching procedure to interpret constant-rate pressure build-up and drawdown data. van Poolen²¹ demonstrated the application of the type-curve procedure in analyzing flow-rate data obtained from an oil well producing with a constant pressure at the well bore. All of his data, however, were in the early transient period. No depletion was evident in his examples. This same type-curve matching procedure can be used for decline-curve analysis.

The basic steps used in type-curve matching declining rate-time data is as follows:

1. Plot the actual rate versus time data in any convenient units on log-log tracing paper of the same size cycle as the type curve to be used. (For convenience all type curves should be plotted on the same log-log scale so that various solutions can be tried.)

2. The tracing paper data curve is placed over a type curve, the coordinate axes of the two curves being kept parallel and shifted to a position which represents the best fit of the data to a type curve. More than one of the type curves presented in this paper may have to be tried to obtain a best fit of all the data.

3. Draw a line through and extending beyond the rate-time data overlain along the uniquely matched type curve. Future rates are then simply read from the real-time scale on which the rate data is plotted.

4. To evaluate decline-curve constants or reservoir variables, a match point is selected anywhere on the overlapping portion of the curves and the coordinates of this

common point on both sheets are recorded.

5. If none of the type curves will reasonably fit all the data, the departure curve method^{15, 22} should be attempted. This method assumes that the data is a composite of two or more different decline-curves. After a match of the late time data has been made, the matched curve is extrapolated backwards in time and the departure, or difference, between the actual rates and rates determined from the extrapolated curve at corresponding times is replotted on the same log-log scale. An attempt is then made to match the departure curve with one of the type curves. (At all times some consideration of the type of reservoir producing mechanism should be considered.) Future predictions should then be made as the sum of the rates determined from the two (or more if needed) extrapolated curves.

TYPE CURVE MATCHING EXAMPLES

Several examples will be presented to illustrate the method of using type curve matching to analyze typical declining rate-time data. The type curve approach provides unique solutions upon which engineers can agree, or shows when a unique solution is not possible with a type curve only. In the event of a non-unique solution, a most probable solution can be obtained if the producing mechanism is known or indicated.

ARPS' HYPERBOLIC DECLINE EXAMPLE

Fig. 10 illustrates a type curve match of Arps' example of hyperbolic decline⁴. Every single data point falls on the $b = 0.5$ type curve. This match was found to be unique in that the data would not fit any other value of "b". Future producing rates can be read directly from the real-time scale on which the data is plotted. If we wish to determine q_i and D_i , use the match points indicated on Fig. 10 as follows

$$q_{Dd} = 0.33 = \frac{q(t)}{q_i} = \frac{1000 \text{ BOPM}}{q_i}$$

$$q_i = \frac{1000 \text{ BOPM}}{0.33} = 30,303 \text{ BOPM}$$

$$t_{Dd} = 12.0 = D_i t = D_i 100 \text{ MO.}$$

$$D_i = \frac{12.0}{100 \text{ MO}} = 0.12 \text{ MO.}^{-1}$$

The data could have also been matched using the type curves on Figs. 6 and 7. In both cases the match would have been obtained with a back-pressure curve slope $n = 0.5$ which

is equivalent to $b = 0.5$. Match points determined from these curves could have been used to calculate q_i and q_i/N_{pi} and finally N_{pi} .

The fact that this example was for a lease, a group of wells, and not an individual well raises an important question. Should there be a difference in results between analyzing each well individually and summing the results, or simply adding all wells production and analyzing the total lease production rate? Consider a lease or field with fairly uniform reservoir properties, "b" or n is similar for each well, and all wells have been on decline at a similar terminal wellbore pressure, p_{wf} , for a sufficient period of time to reach pseudo-steady state. According to Matthews et al.²³ "at (pseudo) steady state the drainage volumes in a bounded reservoir are proportional to the rates of withdrawal from each drainage volume." It follows then that the ratio q_i/N_{pi} will be identical for each well and thus the sum of the results from each well will give the same results as analyzing the total lease or field production rate. Some rather dramatic illustrations of how rapidly a readjustment in drainage volumes can take place by changing the production rate of an offset well or drilling an offset well is illustrated in a paper by Marsh²⁴. Similar drainage volume readjustments in gas reservoirs have also been demonstrated by Stewart²⁵.

For the case where some wells are in different portions of a field separated by a fault or a drastic permeability change, readjustment of drainage volumes proportional to rate cannot take place among all wells. The ratio q_i/N_{pi} may then be different for different group of wells. A total lease or field production analysis would then give different results than summing the results from individual well analysis. A similar situation can also exist for production from stratified reservoirs 26, 27, (no-crossflow).

ARPS' EXPONENTIAL DECLINE EXAMPLE

Fig. 11 shows the results of a type curve analysis of Arps' example of a well with an apparent exponential decline. In this case, there is not sufficient data to uniquely establish a value of "b". The data essentially fall in the region of the type curves where all curves coincide with the exponential solution. As shown on Fig. 11 a value of $b = 0$, (exponential) or $b = 1.0$ (harmonic) appear to fit the data equally well. (Of course all values in between would also fit the data.) The difference in forecasted results from the two extreme interpretations would be great in later years. For an economic limit of 20 BOPM,

the exponential interpretation gives a total life of 285 MONTHS, the harmonic 1480 MONTHS. This points out yet a further advantage of the type curve approach, all possible alternate interpretations can be conveniently placed on one curve and forecasts made from them. A statistical analysis would of course yield a single answer, but it would not necessarily be the correct or most probable solution. Considering the various producing mechanisms we could select.

- $b = 0$, (exponential), if the reservoir is highly undersaturated.
- $b = 0$, (exponential), gravity drainage with no free surface²⁸.
- $b = 0.5$, gravity drainage with a free surface²⁸.
- $b = 0.667$, solution-gas drive reservoir, ($n = 1.0$) if \bar{p}_R vs. N_p is linear.
- $b = 0.333$, solution-gas drive reservoir, ($n = 1.0$) if \bar{p}_R^2 vs. N_p is approximately linear.

FRACTURED WELL EXAMPLE

Fig. 12 is an example of type curve matching for a well with declining rate data available both before and after stimulation. (The data was obtained from Ref. 1.) This type problem usually presents some difficulties in analysis. Both before and after frac. log-log plots are shown on Fig. 12 with the after frac. data reinitialized in time. These before and after log-log plots will exactly overlay each other indicating that the value of "b" did not change for the well after the fracture treatment. (The before frac. plot can be considered as a type curve itself and the after frac. data overlaid and matched on it.) Thus all the data were used in an attempt to define "b". When a match is attempted on the Arps unit solution type curves, it was found that a "b" of between 0.6 and 1.0 could fit the data. Assuming a solution-gas drive, a match of the data was made on the Fig. 6 type curve with $n = 1.0$, $b = 0.667$.

Using the match points for the before frac. data we have from the rate match point,

$$q_{Dd} = 0.243 = \frac{q(t)}{q_{oi}} = \frac{1000 \text{ BOPM}}{q_{oi}}$$

$$q_{oi} = \frac{1000 \text{ BOPM}}{.243} = 4115 \text{ BOPM}$$

From the time match point,

$$t_{Dd} = 0.60 = \left(\frac{q_{oi}}{N_{pi}} \right) t = \frac{(4115 \text{ BOPM})(100 \text{ MO})}{N_{pi}}$$

$$N_{pi} = \frac{(4115 \text{ BOPM})(100 \text{ MO.})}{0.60} = 685,833 \text{ BBL}$$

then

$$\frac{q_{oi}}{N_{pi}} = \frac{4115 \text{ BOPM}}{685,833} = .006000 \text{ MO.}^{-1}$$

Now using the match points for the after frac. data we have from the rate match point,

$$q_{Dd} = 0.134 = \frac{q(t)}{q_{oi}} = \frac{1000 \text{ BOPM}}{q_{oi}}$$

$$q_{oi} = \frac{1000 \text{ BOPM}}{0.134} = 7463 \text{ BOPM}$$

From the time match point

$$t_{Dd} = 1.13 = \left(\frac{q_{oi}}{N_{pi}} \right) t = \frac{(7463 \text{ BOPM})(100 \text{ MO.})}{N_{pi}}$$

$$N_{pi} = \frac{(7463 \text{ BOPM})(100 \text{ MO.})}{1.13} = 660,442 \text{ BBL}$$

then

$$\frac{q_{oi}}{N_{pi}} = \frac{7463 \text{ BOPM}}{660,442 \text{ BBL}} = .011300 \text{ MO.}^{-1}$$

We can now check the two limiting conditions to be considered following an increase in rate after a well stimulation. They are:

1. Did we simply obtain an acceleration of production, the wells reserves remaining the same?

2. Did the reserves increase in direct proportion to the increase in producing rate as a result of a radius of drainage readjustment²³? Before treatment, N_{pi} was found to be 685,833 BBL. Cumulative production determined from the rate data prior to stimulation was 223,500 BBL. N_{pi} then at the time of the fracture treatment is

$$N_{pi} = 685,833 \text{ EBL} - 223,500 \text{ BBL} = 462,333 \text{ BBL}$$

If only accelerated production was obtained and the reserve remained the same, $\frac{q_i}{N_{pi}}$ after

the fracture treatment should have been

$$\frac{7463 \text{ BOPM}}{462,333 \text{ BBL}} = 0.016142 \text{ MO.}^{-1}$$

Actual (q_{oi}/N_{pi}) after treatment was 0.011300 MO.^{-1} . If the reserves increased in direct

proportion to the flow-rate, the ratio q_{oi}/N_{pi} should have remained the same as that obtained prior to treatment or 0.006000 MO.^{-1} . This then would have indicated an N_{pi} of

$$N_{pi} = \frac{7463 \text{ BOPM}}{.006000 \text{ MO.}^{-1}} = 1,243,833 \text{ BBL}$$

Actual increase in reserves as a result of the fracture treatment appears to lie between the two extremes. Based on the method of analysis used, the actual increase in reserves attributable to the fracture treatment is 198,109 BBL, (660,442 BBL - 462,333 BBL).

STRATIFIED RESERVOIR EXAMPLE

This example illustrates a method of analyzing decline-curve data for a layered (no-crossflow) or stratified reservoir using type curves. The data is taken from Ref. 18 and is for the East Side Colinga Field. Ambrose²⁹ presented a cross section of the field showing an upper and lower oil sand separated by a continuous black shale. This layered description for the field along with the predictive equation for stratified reservoir presented in Ref. 29 led to the idea of using the departure curve method (differencing) to analyzed decline-curve data.

After Russell and Prats²⁷, the production rate of a well (or field) at pseudo-steady state producing a single phase liquid at the same constant wellbore pressure, ($r_{wf} = 0$ for simplicity), from two stratified layers is

$$q_T(t) = q_{i1} e^{-\left(\frac{q_i}{N_{pi}}\right)_1 t} + q_{i2} e^{-\left(\frac{q_i}{N_{pi}}\right)_2 t} \dots (35)$$

or

$$q_T(t) = q_1(t) + q_2(t) \dots (36)$$

The total production from both layers then is simply the sum of two separate forecasts. Except for the special case of the ratio q_i/N_{pi} being equal for both layers, the sum of two exponentials will not in general result in another exponential.

In attempting to match the rate-time data to a type curve, it was found that the late time data can be matched to the exponential ($b = 0$) type curve. Fig. 13 shows this match of the late time data designated as layer 1. With this match, the curve was extrapolated backwards in time and the departure, or difference, between the actual rates determined from the extrapolated curve was replotted on the same log-log scale. See TABLE 1 for a

summary of the departure curve results. The difference or first departure curve, layer 2, itself resulted in a unique fit of the exponential type curve, thus satisfying Eq. 35 which can now be used to forecast the future production. Using the match points indicated on Fig. 13 to evaluate q_1 and D_1 for each layer the predictive equation becomes

$$q_T(t) = 58,824 \text{ BOPY } e^{- (0.200)t} + 50,000 \text{ BOPY } e^{- (0.535)t}$$

where t is in years.

Higgins and Lechtenberg³⁰ named the sum of two exponentials the double semilog. They reasoned that the degree of fit of empirical data to an equation increases with the number of constants.

This interpretation is not claimed to be the only interpretation possible for this set of data. A match with $b = 0.2$ can be obtained fitting nearly all of the data points but can not be explained by any of the drive mechanisms so far discussed. The layered concept fits the geologic description and also offered the opportunity to demonstrate the departure curve method. The departure curve method essentially places an infinite amount of combinations of type curves at the disposal of the engineer with which to evaluate rate-time data.

EFFECT OF A CHANGE IN BACK-PRESSURE

The effect of a change in back-pressure is best illustrated by a hypothetical single well problem. The reservoir variables and conditions used for this example are given in Table 2. The analytical single-phase liquid solution of Fig. 3 is used to illustrate a simple graphical forecasting superposition procedure. The inverse procedure, the departure or differencing method can be used to analyze decline-curve data affected by back-pressure changes.

After Hurst¹², superposition for the constant-pressure case for a simple single pressure change can be expressed by

$$q(t) = \frac{kh (p_i - p_{wf1})}{141.3(\mu B) \left[\ln \left(\frac{r_e}{r_w} \right) - \frac{1}{2} \right]} q_{Dd}(t_{Dd}) + \frac{kh (p_{wf1} - p_{wf2})}{141.3(\mu B) \left[\ln \left(\frac{r_e}{r_w} \right) - \frac{1}{2} \right]} q_{Dd}(t_{Dd} - t_{Dd1})$$

or

$$q(t) = \frac{kh (p_i - p_{wf1})}{141.3(\mu B) \left[\ln \left(\frac{r_e}{r_w} \right) - \frac{1}{2} \right]} \cdot \left[q_{Dd}(t_{Dd}) + \frac{p_{wf1} - p_{wf2}}{p_i - p_{wf1}} q_{Dd}(t_{Dd} - t_{Dd1}) \right] \dots \dots \dots (37)$$

Up to the time of the pressure change p_{wf2} at t_{Dd1} the well production is simply q_1 as depicted on Fig. 14. The q_1 forecast as a function of time is simply made by evaluating a single set of match points using the reservoir variables given in Table 2. At p_{wf1} and $r_e/r'_w = 100$

$$t = 1 \text{ DAY}; t_{Dd} = 0.006967$$

$$q_1(t) = 697 \text{ BOPD}; q_{Dd} = 2.02$$

Plot the rate 697 BOPD and time of 1 day on log-log tracing paper on the same size cycle as Fig. 3. Locate the real-time points over the dimensionless time points on Fig. 3 and draw in the r_e/r'_w curve of 100 on the tracing paper. Read flow rates as a function of time directly from the real time scale.

When a change in pressure is made to p_{wf2} at t_1 , t equal zero for the accompanying change in rate q_2 , (really a Δq for superposition), this rate change retraces the q_{Dd} vs. t_{Dd} curve and is simply a constant fraction of q_1

$$q_2 = q_1 \left[\frac{p_{wf1} - p_{wf2}}{p_i - p_{wf1}} \right]$$

or q_2 at $t - 1$ day after the rate change is equal to

$$q_2 = 697 \text{ BOPD } \frac{1000 \text{ psi} - 50 \text{ psi}}{4000 \text{ psi} - 1000 \text{ psi}} = 221 \text{ BOPD}$$

The total rate q_T after the pressure change is $q_T = q_1 + q_2$ as depicted in Fig. 14. All rates of flow for this example were read directly from the curves on Fig. 14 and summed at times past the pressure change p_{wf2} .

The practical application of this example in decline-curve analysis is that the departure or difference method can be used on rate-time data affected by a change in

back-pressure. The departure curve represented by q_2 on Fig. 14 should exactly overlay the curve represented by q_1 . If it does in an actual field example, the future forecast is correctly made by extending both curves and summing them at times beyond the pressure change.

CALCULATION OF kh FROM DECLINE-CURVE DATA

Pressure build-up and decline-curve data were available from a high-pressure, highly undersaturated, low-permeability sandstone reservoir. Initial reservoir pressure was estimated to be 5790 psia at -9300 ft. with a bubble-point pressure of 2841 psia. Two field-wide pressure surveys were conducted while the reservoir was still undersaturated. Table 3 summarizes the reservoir properties and basic results obtained from the pressure build-up analysis on each well. Note that nearly all wells had negative skins as a result of hydraulic fracture treatments. Also, appearing on this table are results obtained from an attempt to calculate kh using decline-curve data available for each of the wells.

Ten of the twenty-two wells started on decline when they were first placed on production. As a result, the early production decline data existed in the transient period and a type curve analysis using Fig. 3 was matched to one of the r_e/r_w stems. Other wells listed on the table, where an r_e/r_w match is not indicated, were prorated wells and began their decline several months after they were first put on production. For the decline-curve determination of kh, the reservoir pressure existing at the beginning of decline for each well was taken from the pressure history match of the two field-wide pressure surveys. The constant bottom hole flowing pressure for the wells ranged between 800 and 900 psia.

A type curve match using decline-curve data to calculate kh for well No. 13 is illustrated on Fig. 15. A type curve match using pressure build-up data obtained on this same well is illustrated on Fig. 16. The constant-rate type curve of Gringarten et al.⁸ for fractured wells was used for matching the pressure build-up data. The build-up kh of 47.5 md.-ft. compares very well with the kh of 40.5 MD-FT determined by using the rate-time decline-curve data.

In general, the comparison of kh determined from decline-curve data and pressure build-up data tabulated on Table 3 is surprisingly good. (The pressure build-up analysis was performed independently by another engineer.) One fundamental observation to be made from the results obtained on wells where a match of r_e/r_w was not possible is that the effective

wellbore radius r_w' (obtained from the build-up analysis) is used to obtain a good match between build-up and decline-curve calculated kh.

TYPE CURVES FOR KNOWN RESERVOIR AND FLUID PROPERTIES

All the type curves so far discussed were developed for decline-curve analysis using some necessary simplifying assumptions. For specific reservoirs, when PVT data, reservoir variables, and back-pressure tests are available, type curves could be generated for various relative permeability curves and back-pressures. These curves developed for a given field would be more accurate for analyzing decline data in that field. Conventional material balance programs or more sophisticated simulation models could be used to develop dimensionless constant-pressure type curves as was done by Levine and Pratts³¹ (See their Fig. 11).

CONCLUSIONS

Decline-curve analysis not only has a solid fundamental base, but provides a tool with more diagnostic power than has previously been suspected. The type curve approach provides unique solutions upon which engineers can agree, or shows when a unique solution is not possible with a type curve only. In the event of a non-unique solution, a most probable solution can be obtained if the producing mechanism is known or indicated.

NOMENCLATURE

b	=	Reciprocal of decline curve exponent (1/b)
B	=	Formation volume factor, res. vol./surface vol.
c_t	=	Total compressibility, psi^{-1}
C_g	=	Gas well back-pressure curve coefficient
D_i	=	Initial Decline rate, t^{-1}
e	=	Natural logarithm base 2.71828
G	=	Initial gas-in-place, surface measure
G_p	=	Cumulative gas production, surface measure
h	=	Thickness, ft.
J_o	=	Productivity index, STK BBL/DAY/PSI
J'_o	=	Productivity index (back-pressure curve coefficient) STK BBL/DAY/(psi) ²ⁿ
k	=	Effective permeability, md.
n	=	Exponent of back-pressure curve
N_p	=	Cumulative oil production, STK BBL

N_{Fi}	= Cumulative oil production to a reservoir shut-in pressure of 0, STK BBL
P_i	= Initial pressure, psia
\bar{P}_R	= Reservoir average pressure (shut-in pressure), psia
P_{wf}	= Bottom-hole flowing pressure, psia
q_i	= Initial surface rate of flow at $t = 0$
$(q_i)_{max}$	= Initial wide-open surface flow rate at $P_{wf} = 0$
$q(t)$	= Surface rate of flow at time t
q_D	= Dimensionless rate, (Eq. 6)
q_{Dd}	= Decline curve dimensionless rate, (Eq. 4)
Q_D	= Dimensionless cumulative production
r_e	= External boundary radius, ft.
r_w	= Wellbore radius, ft.
r'_w	= Effective wellbore radius, ft.
t	= Time, (Days for t_D)
t_D	= Dimensionless time, (Eq. 7)
t_{Dd}	= Decline curve dimensionless time, (Eq. 5)
ϕ	= Porosity, fraction of bulk volume
μ	= Viscosity, cp.

REFERENCES

- Ramsay, H. J., Jr.: "The Ability of Rate-Time Decline Curves to Predict Future Production Rates", M.S. Thesis, U. of Tulsa, Tulsa, Okla. (1968).
- Slider, H. C.: "A Simplified Method of Hyperbolic Decline Curve Analysis", J. Pet. Tech. (March, 1968), 235.
- Gentry, R. W.: "Decline-Curve Analysis", J. Pet. Tech. (Jan., 1972) 38.
- Arps, J. J.: "Analysis of Decline Curves", Trans. AIME (1945) 160, 228.
- Ramey, H. J., Jr.: "Short-Time Well Test Data Interpretation in the Presence of Skin Effect and Wellbore Storage", J. Pet. Tech. (Jan., 1970) 97.
- Agarwal, R., Al-Hussainy, R. and Ramey, H. J., Jr.: "An Investigation of Wellbore Storage and Skin Effect in Unsteady Liquid Flow: I. Analytical Treatment", Soc. Pet. Eng. J. (Sept., 1970) 279.
- Raghavan, R., Gady, G. V. and Ramey, H. J., Jr.: "Well-Test Analysis for Vertically Fractured Wells", J. Pet. Tech. (Aug. 1972) 1014.
- Gringarten, A. C., Ramey, H. J., Jr. and Raghavan, R.: "Pressure Analysis for Fractured Wells", Paper SPE 4051 presented at the 47th Annual Fall Meeting, San Antonio, Texas, (Oct 8-11, 1972).
- McKinley, R. M.: "Wellbore Transmissibility from Afterflow-Dominated Pressure Buildup Data", J. Pet. Tech. (July, 1971) 863.
- Moore, T. V., Schilthuis, R. J. and Hurst, W.: "The Determination of Permeability from Field Data", Bull. API (May, 1933) 211, 4.
- Hurst, W.: "Unsteady Flow of Fluids in Oil Reservoirs", Physics, (Jan., 1934) 5, 20.
- Hurst, W.: "Water Influx into a Reservoir and Its Application to the Equation of Volumetric Balance", Trans., AIME (1943) 151, 57.
- van Everdingen, A. F. and Hurst, W.: "The Application of the Laplace Transformation to Flow Problems in Reservoirs", Trans. AIME (1949) 186, 305.
- Fetkovich, M. J.: "The Isochronal Testing of Oil Wells", Paper SPE 4529 presented at the 48th Annual Fall Meeting, Las Vegas, Nevada, (Sept. 30-Oct. 3, 1973).
- Ferris, J., Knowles, D. B., Brown, R. H., and Stallman, R. W.: "Theory of Aquifer Tests", U. S. Geol. Surv., Water Supply Paper 1536E (1962), 109.
- Tsarevich, K. A. and Kuranov, I. F.: "Calculation of the Flow Rates for the Center Well in a Circular Reservoir Under Elastic Conditions", Problems of Reservoir Hydrodynamics Part I, Leningrad, (1966), 9-34.
- Fetkovich, M. J.: "A Simplified Approach to Water Influx Calculations-Finite Aquifer Systems", J. Pet. Tech. (July, 1971) 814.
- Cuttler, W. W., Jr.: "Estimation of Underground Oil Reserves by Oil-Well Production Curves", Bull., USBM (1924) 228.
- Stewart, P. R.: "Low-Permeability Gas Well Performance at Constant Pressure", J. Pet. Tech. (Sept. 1970) 1149.

20. Gurley, J.: "A Productivity and Economic Projection Method-Ohio Clinton Sand Gas Wells", Paper SPE 686 presented at the 38th Annual Fall Meeting, New Orleans, La., (Oct. 6-9, 1963).
21. van Poollen, H. K.: "How to Analyze Flowing Well-Test Data... with Constant Pressure at the Well Bore", Oil and Gas Journal (Jan. 16, 1967).
22. Witherspoon, P. A., Javandel, I., Neuman, S. P. and Freeze, P. A.: "Interpretation of Aquifer Gas Storage Conditions from Water Pumping Tests", Monograph AGA, New York (1967) 110.
23. Matthews, C. S., Brons, F. and Hazebroek, P.: "A Method for Determination of Average Pressure in a Bounded Reservoir", Trans., AIME (1954) 201, 182.
24. Marsh, H. N.: "Method of Appraising Results of Production Control of Oil Wells", Bull., API (Sept., 1928) 202, 86.
25. Stewart, P. R.: "Evaluation of Individual Gas Well Reserves", Pet. Eng. (May, 1966) 85.
26. Lefkovits, H. C. and Matthews, C. S.: "Application of Decline Curves to Gravity-Drainage Reservoirs in the Stripper Stage", Trans., AIME (1958) 213, 275.
27. Russel, D. G. and Prats, M.: "Performance of Layered Reservoirs with Crossflow--- Single-Compressible Fluid Case", Soc. Pet. Eng. J. (March, 1962) 53.
28. Matthews, C. S. and Lefkovits, H. C.: "Gravity Drainage Performance of Depletion-Type Reservoirs in the Stripper Stage", Trans., AIME (1956) 207, 265.
29. Ambrose, A. W.: "Underground Conditions in Oil Fields", Bull., USBM (1921) 195, 151.
30. Higgins, R. V. and Lechtenberg, H. J.: "Merits of Decline Equations Based on Production History of 90 Reservoirs", Paper SPE 2450 presented at the Rocky Mt. Regional Meeting, Denver, Colo., (May 25-27, 1969).
31. Levine, J. S. and Prats, M.: "The Calculated Performance of Solution-Gas Drive Reservoirs", Soc. Pet. Eng. J. (Sept., 1961) 142.

ACKNOWLEDGEMENT

I wish to thank Phillips Petroleum Co. for permission to publish this paper.

NOTE: The author has a limited quantity of full size type curves with grid suitable for actual use which are available on written request.

TABLE 1 - SUMMARY OF RATE-TIME DATA FROM EAST SIDE COALFIELD FIELD¹ WITH THE RESULTS FROM THE DEPARTURE CURVE METHOD

Time Yrs.	(1) Total Field Rate-q _T BOFY	(2) Layer 1 Rate-q ₁ BOFY	(1)-(2) Layer 2 Rate-q ₂ BOFY
0.5	90,000	52,000*	38000
1.5	64,000	42,500*	21500
2.5	48,000	34,500*	13500
3.5	36,000	28,500*	7500
4.5	27,500	23,000*	4500
5.5	21,250	18,600*	2650
6.5	16,250	15,000*	1250
7.5	12,000	12,500*	500
8.5	10,500	10,500	0
9.5	8,500	8,500	
10.5	6,500	6,500	
11.5	5,600	5,600	
12.5	4,550	4,550	
13.5	3,800	3,800	
14.5	3,200	3,200	
15.5	2,750	2,750	

* Taken from layer 1 curve Fig. 13.

TABLE 2 - DATA FOR EXAMPLE PROBLEM OF A DUAL-LAYER RESERVOIR

$I_2 = 4000 \text{ psia}$
 $I_{wf(1)} = 1000 \text{ psia}$
 $I_{wf(2)} = 50 \text{ psia}$
 $k = 1 \text{ md}$
 $h = 100 \text{ FT}$
 $u_o = 1 \text{ cP}$
 $B_o = 1.50 \text{ RES IBL/STE BBL}$
 $z_t = 20 \times 10^{-6} \text{ (SI)}^{-1}$
 $r_e = 1053 \text{ FT. (80 acres)}$
 $r_w' = 10.53 \text{ FT (stimulated well)}$
 $t_D = \frac{0.00134 \mu t}{\phi \mu z_t r_w'^2} = \frac{0.00134 (1) t}{(0.2)(1.0)(20 \times 10^{-6})(10.53)^2} = 14.30 t$
 $t_{UD} = \frac{14.30^2 t}{2.3(0.2) \ln(10.53/0.5)} = 0.00097 t \text{ Days}$
 $q_{UD} = \frac{q(t)}{2.3(F_1 - I_{wf})} = \frac{q(t)}{2.3(1000 - 50)} = \frac{q(t)}{2345}$
 $q(t) = 2345 q_{UD}(t)$ or $q(t) = 2.00(2345) q_{UD}(t)$
 $q(t) = 4690 \text{ BOFY}$

TABLE 3 - PRESSURE BUILD-UP RESULTS FOR THE 22 WELLS IN THE EAST SIDE COALFIELD FIELD

Well No.	h, FT.	c	swe	Pressure Build-up Results		
				Skin	r _{w'} , FT.	h _r , MD, FT.
1	34	9.4	37.9	-0.23	0.3	170.5
2	120	10.5	12.3	-2.65	3.5	56.7
3	32	9.9	20.4	-3.71	10.3	63.0
4	63	9.5	18.6	-3.41	7.6	28.5
5	67	10.2	15.1	-4.29	18.3	44.4
6	78	10.3	12.6	-2.67	2.0	57.9
7	17	10.0	17.5	-2.41	7.0	14.8
8	47	9.1	24.2	-3.74	10.0	16.6
9	87	10.2	18.0	-4.14	16.5	104.7
10	40	10.4	21.7	-5.88	82.9	363.2
11	27	11.5	19.2	-1.00	2.0	59.9
12	19	11.1	17.0	-3.97	13.3	8.9
13	121	10.1	18.8	-3.85	11.8	47.5
14	71	9.4	20.4	-4.10	15.0	224.8
15	49	10.9	28.6	-3.59	9.1	101.9
16	35	10.0	25.6	-4.57	24.2	14.3
17	62	8.8	22.4	-3.12	5.7	27.2
18	75	9.4	18.1	-1.50	1.2	65.1
19	38	3.9	19.2	-2.11	2.1	40.5
20	60	9.6	24.6	-5.48	60.1	88.1
21	56	11.1	16.5	-2.15	2.2	39.1
22	40	8.9	22.5	-3.79	11.1	116.0

* r_{w'} used from build-up analysis with r_e of 1050 ft.

TABLE 4 - DEPARTURE CURVE ANALYSIS RESULTS

r _{w'} , FT.	Matched	Departure Curve Analysis Results			
		q _{UD} , 10,000 BOFY	14 - I _{wf} / (u _o F _o)	h _r , MD-FT	h, MD
34	*	.52	6658	108	3.18
120	*	.68	7979	40	0.38
32	*	.43	2547	0	0.00
63	40	.58	8273	30	0.40
67	70	.57	6796	30	0.40
78	*	.60	7624	0	0.00
17	10	1.30	7781	7.4	0.40
47	10	1.14	7325	10	0.40
87	*	.435	5642	70	0.70
40	*	.36	1211	155	0.30
27	*	.56	7009	60	0.60
19	50	3.30	5045	9.5	0.50
121	50	.54	7259	40.5	0.33
71	*	.32	5737	104	1.40
49	*	.43	4312	110	1.30
35	20	.90	5110	24	0.60
62	*	.82	8198	30	0.50
75	*	.52	6344	23	1.20
38	20	.54	6728	32	0.80
60	*	.340	5090	04	1.00
56	20	.72	5428	20	0.50
40	100	.40	8114	50	1.28

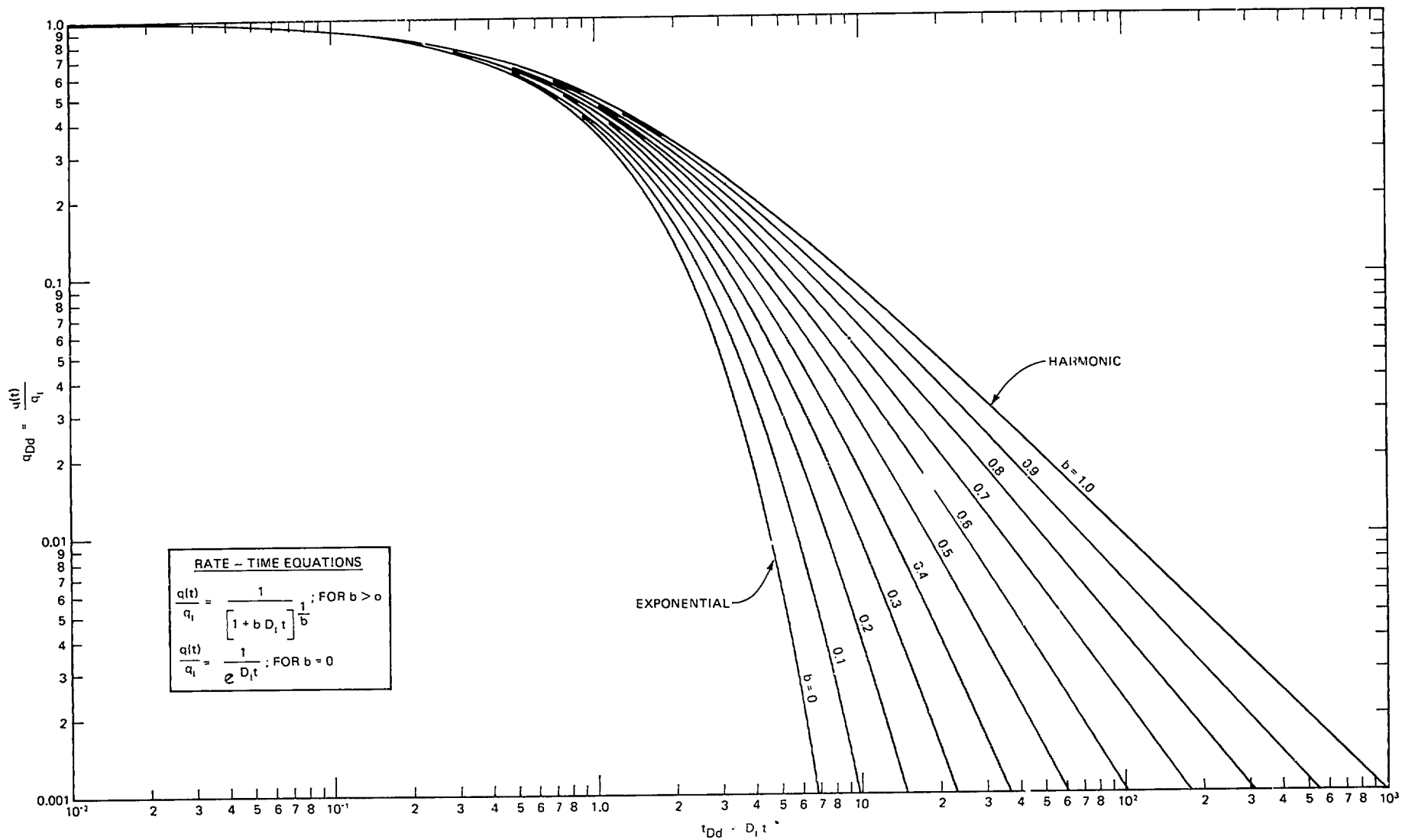


Fig. 1 - Type curves for Arps empirical rate-time decline equations, unit solution ($D_i = 1$).

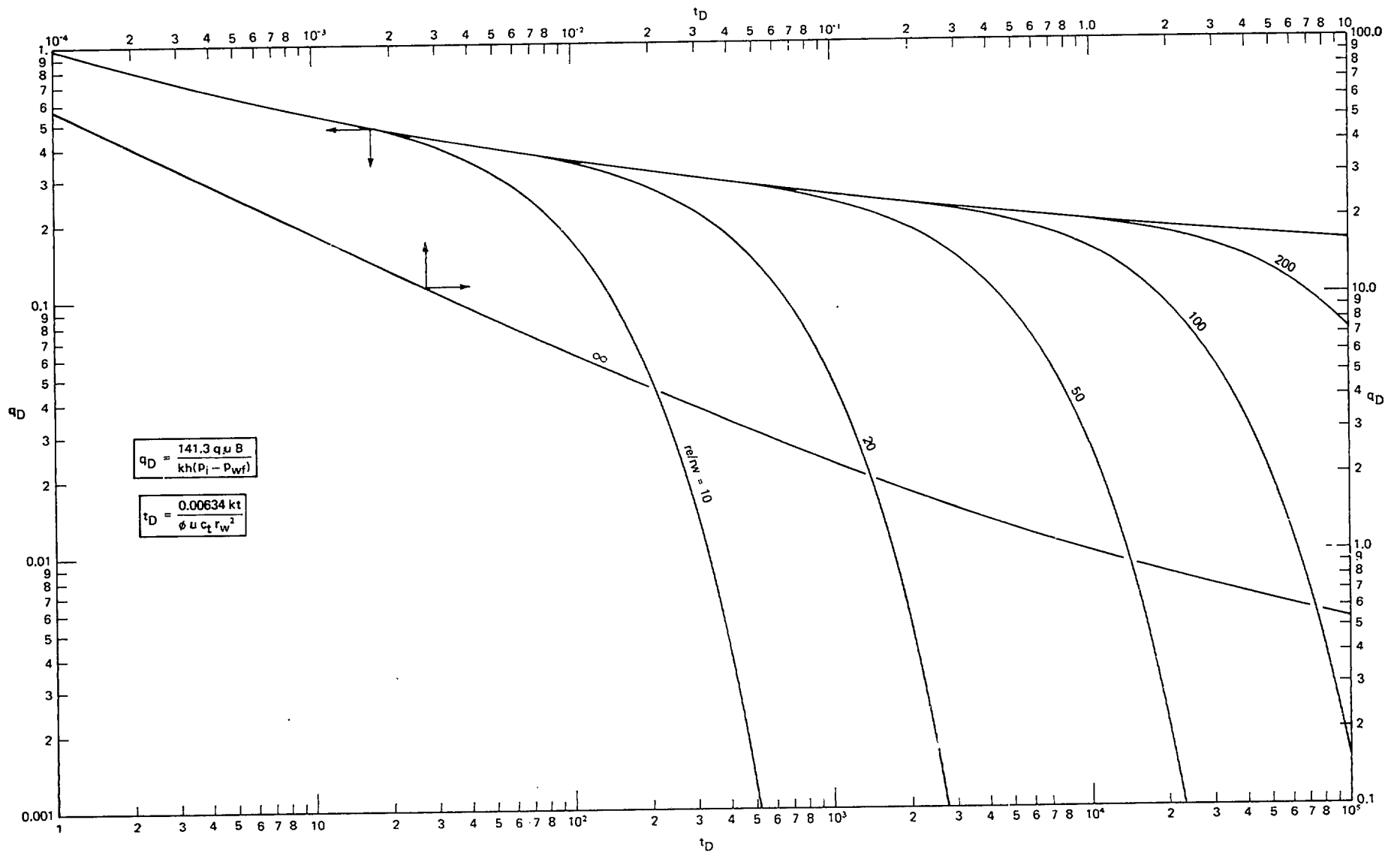


Fig. 2A - Dimensionless flow rate functions plane radial system infinite and finite outer boundary, constant pressure at inner boundary. 10,11,15,16

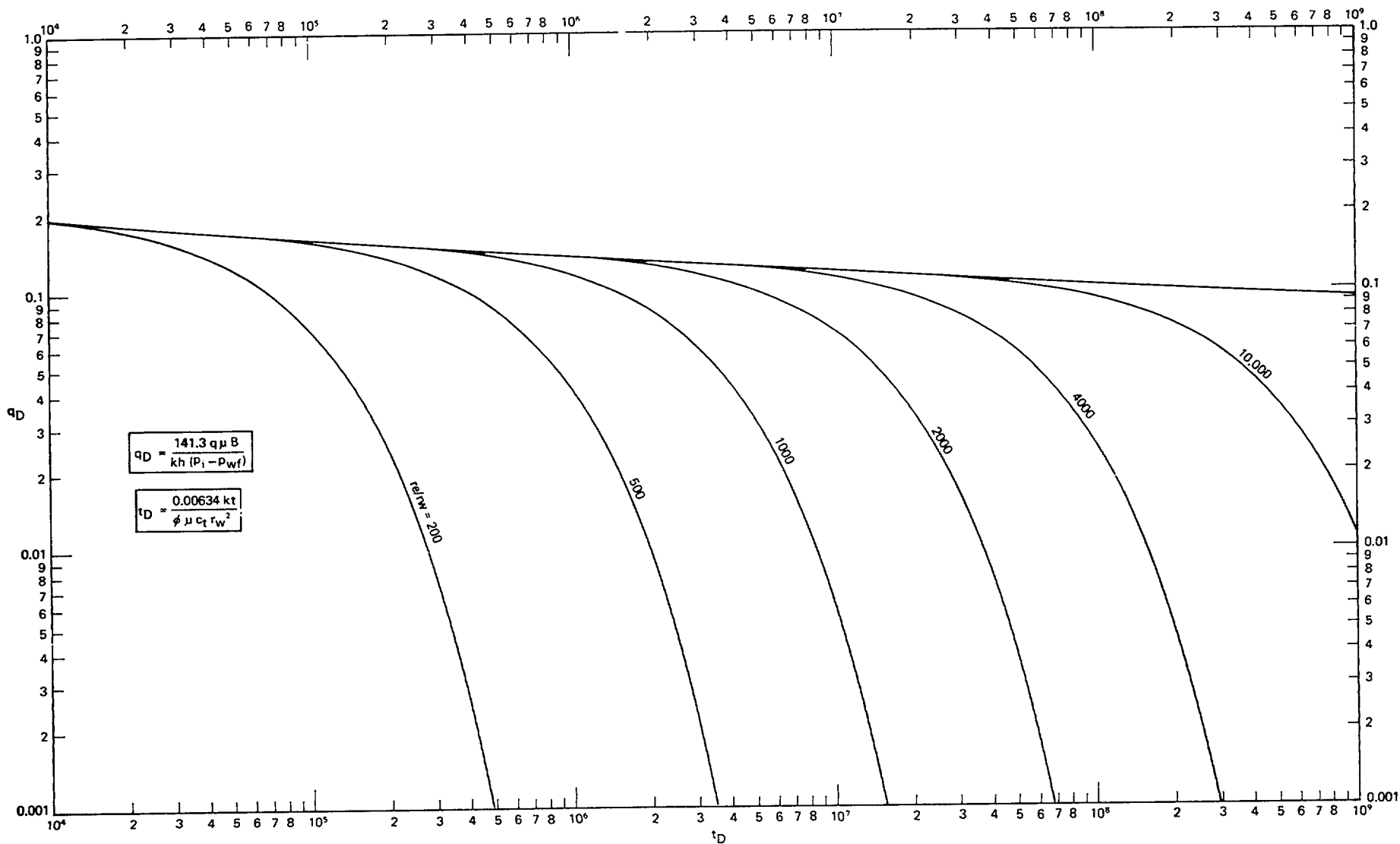


Fig. 2B - Dimensionless flow rate functions plane radial system infinite and finite outer boundary, constant pressure at inner boundary.^{10,11,15,16}

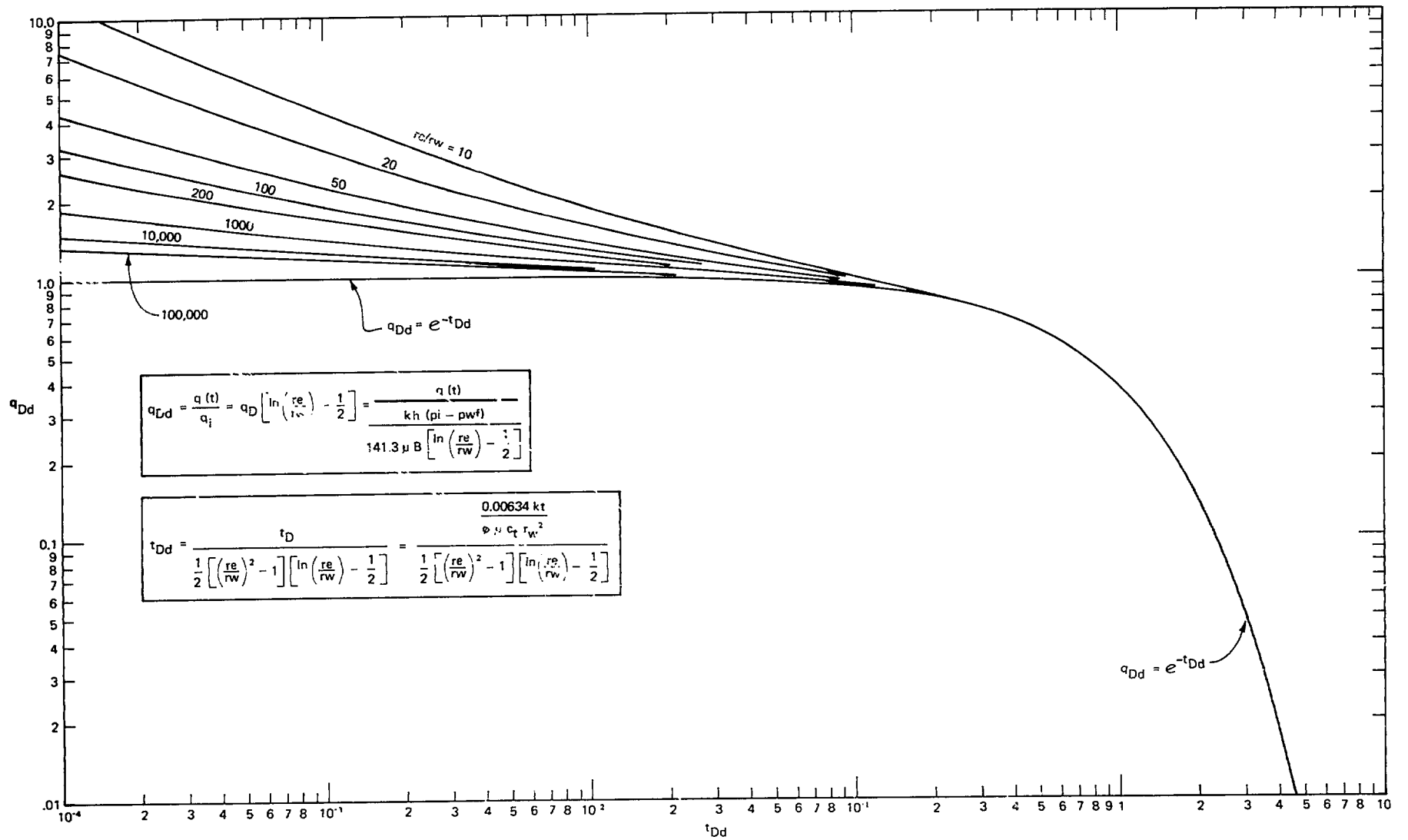


Fig. 3 - Dimensionless flow rate functions for plane radial system, infinite and finite outer boundary, constant pressure at inner boundary.

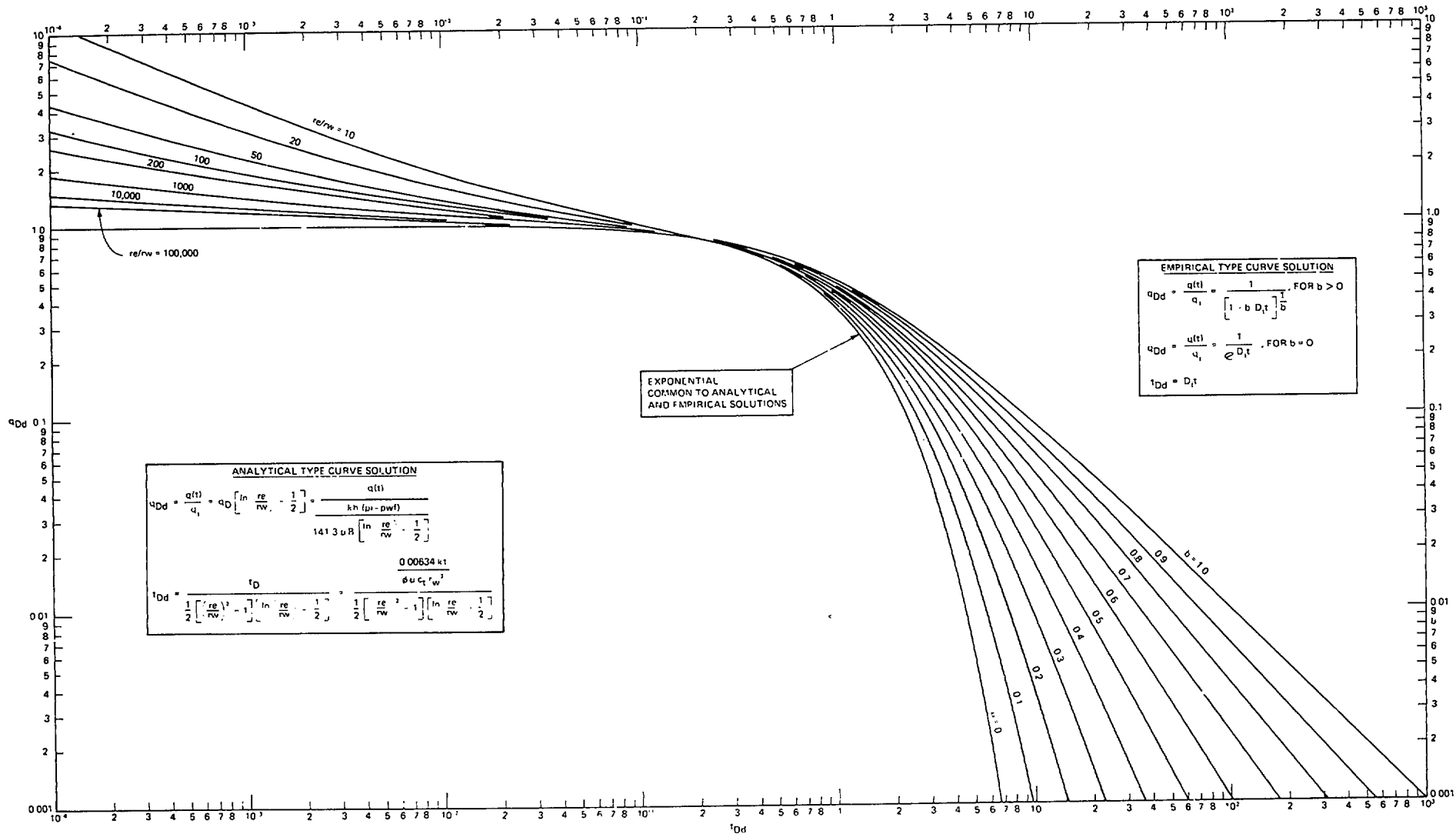


Fig. 4 - Composite of analytical and empirical type curves of Figs. 1 and 3.

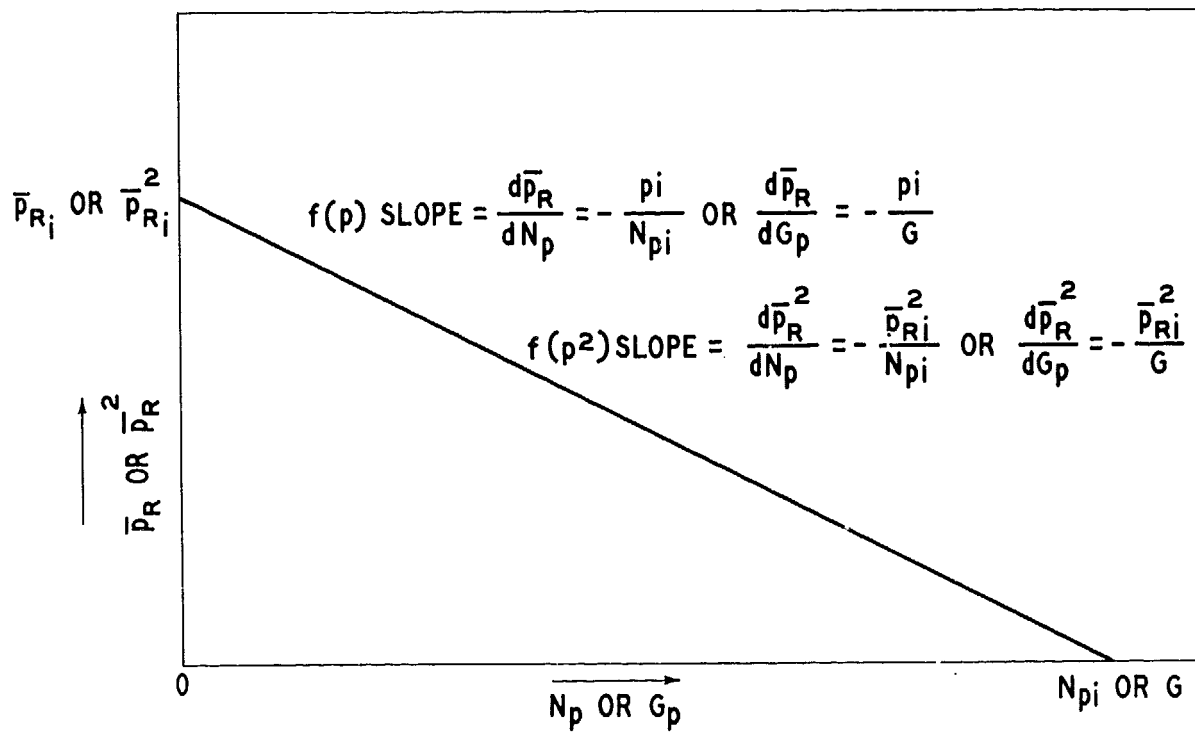


Fig. 5A - Graphical representation of material balance equation.

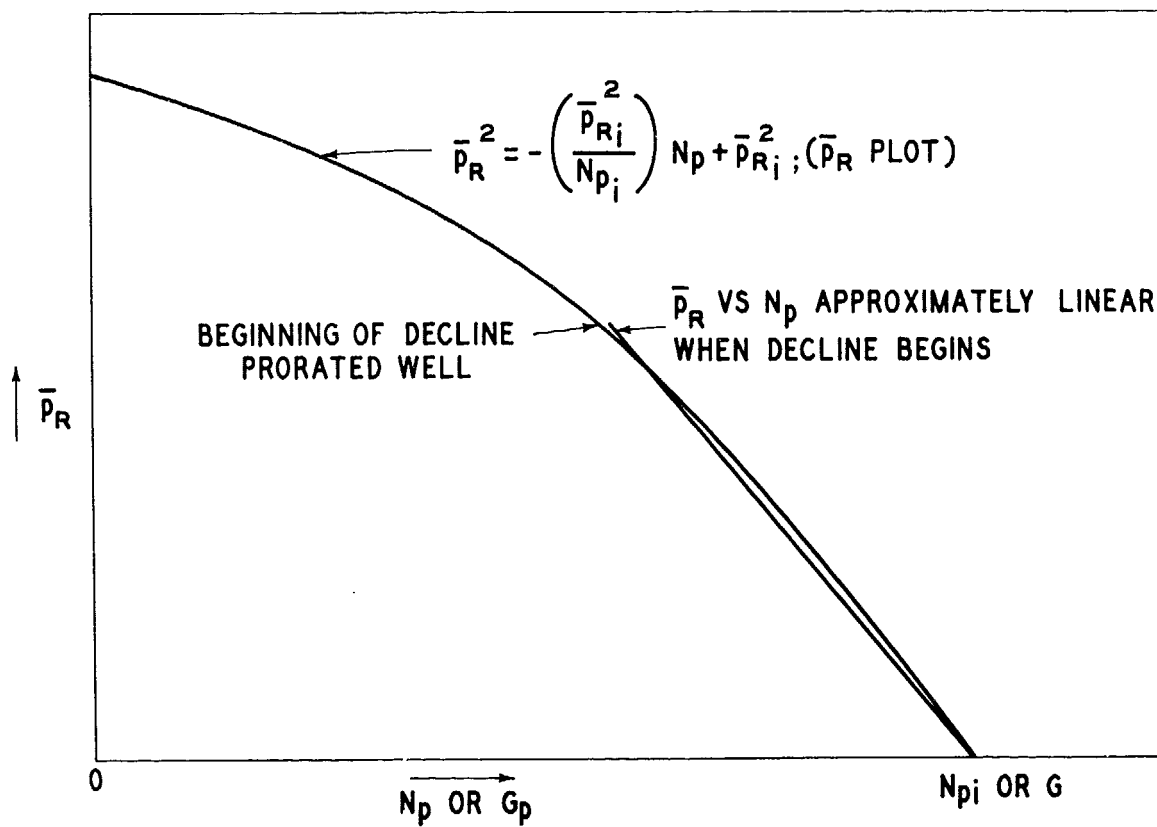


Fig. 5B - Graphical representation of material balance equation.

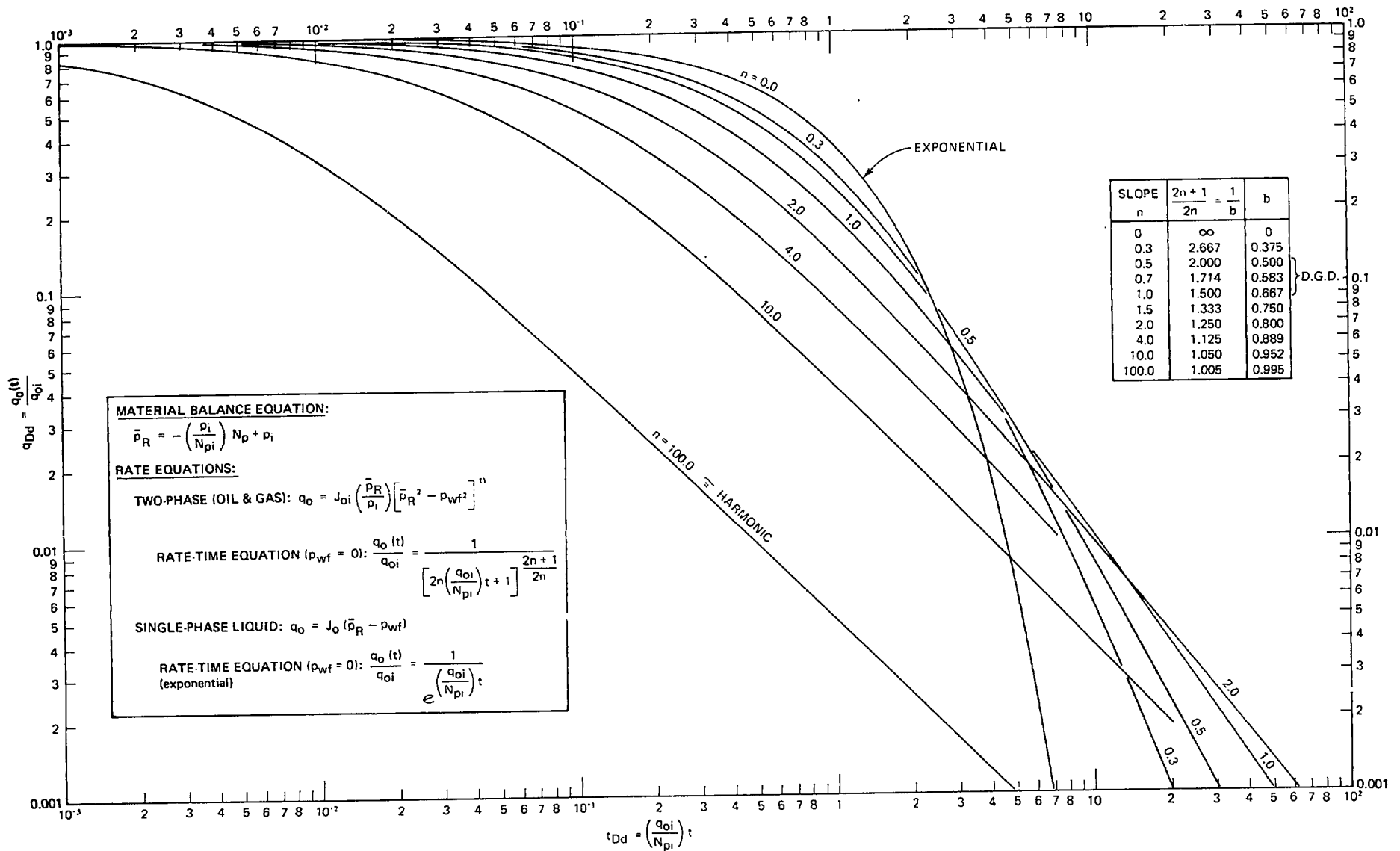


Fig. 6 - Dissolved gas drive reservoir rate - decline type curves finite system with constant pressure at inner boundary ($p_{wf} = 0 @ r_w$). Early transient effects not included.

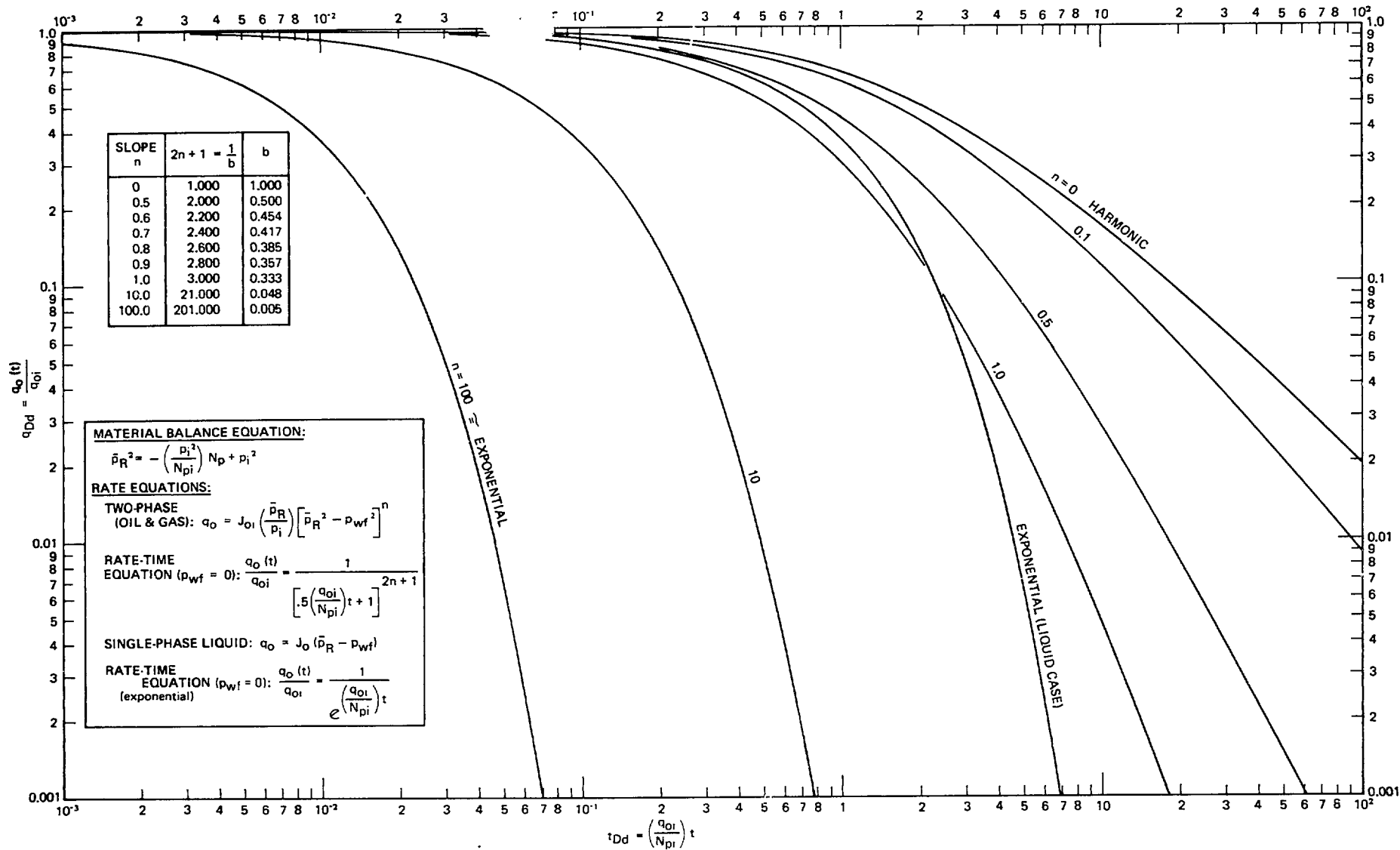


Fig. 7 - Dissolved gas drive reservoir rate - decline type curves finite system with constant pressure at inner boundary ($p_{wf} = 0 @ r_w$). Early transient effects not included.

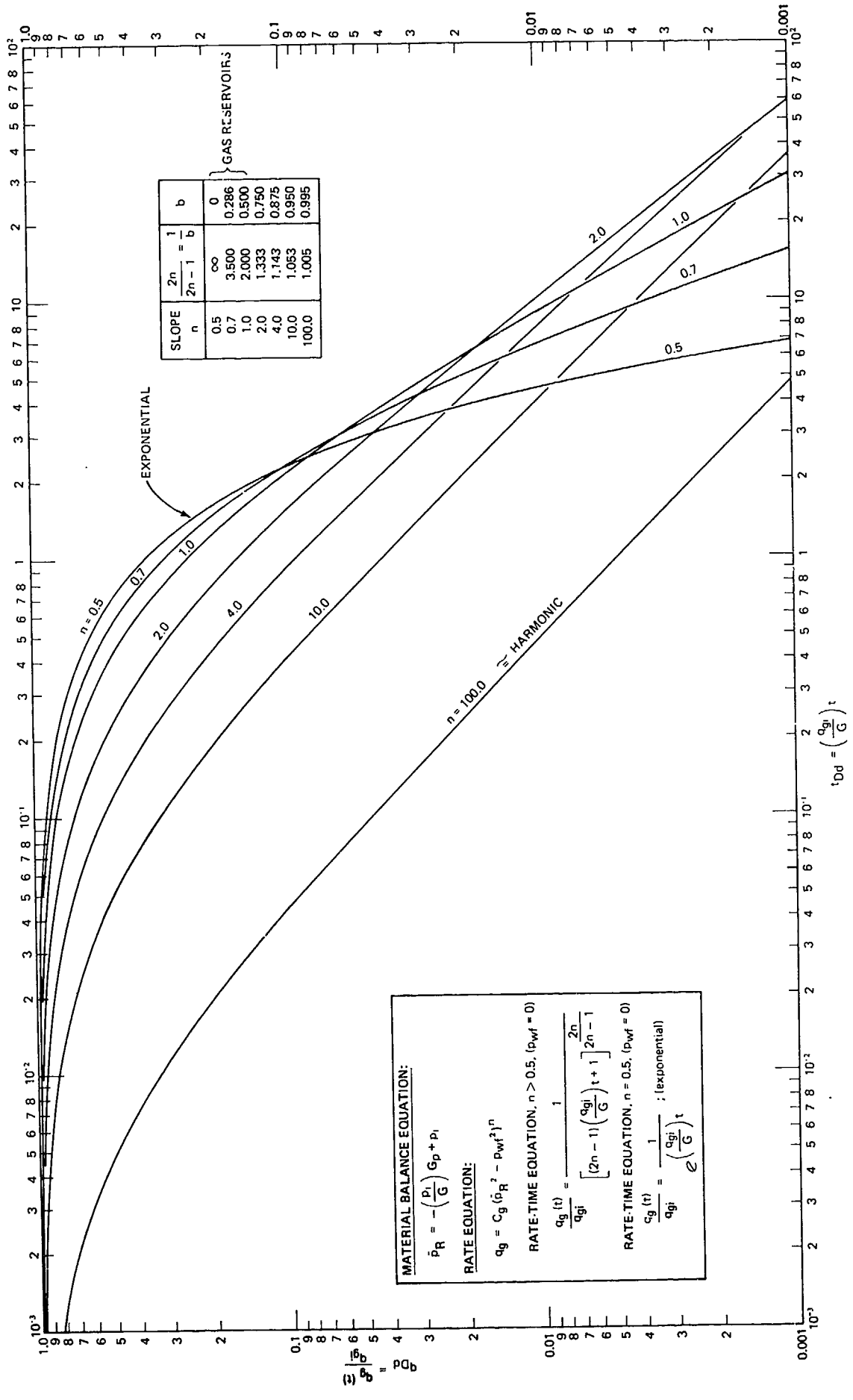


Fig. 8 - Gas reservoir rate - decline type curves finite system with constant pressure at inner boundary ($p_{wf} = 0 @ r_w$). Early transient effects not included.

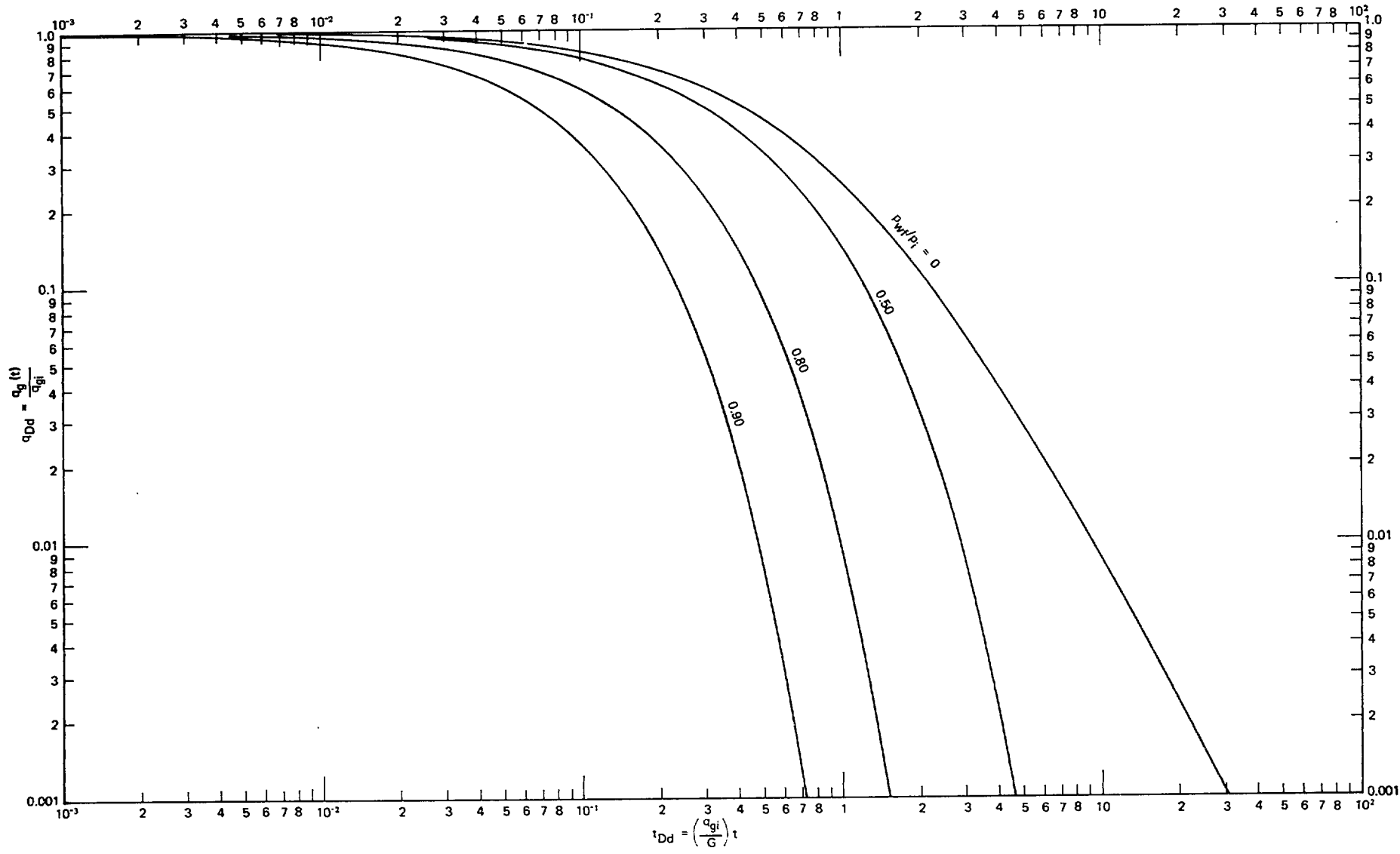


Fig. 9 - Gas reservoir rate decline type curves with back pressure finite system with constant pressure at inner boundary ($p_{wf} = \text{constant} @ r_w$). Early transient effects not included and $z = 1$ (based on gas well back pressure curve slope, $n = 1$).

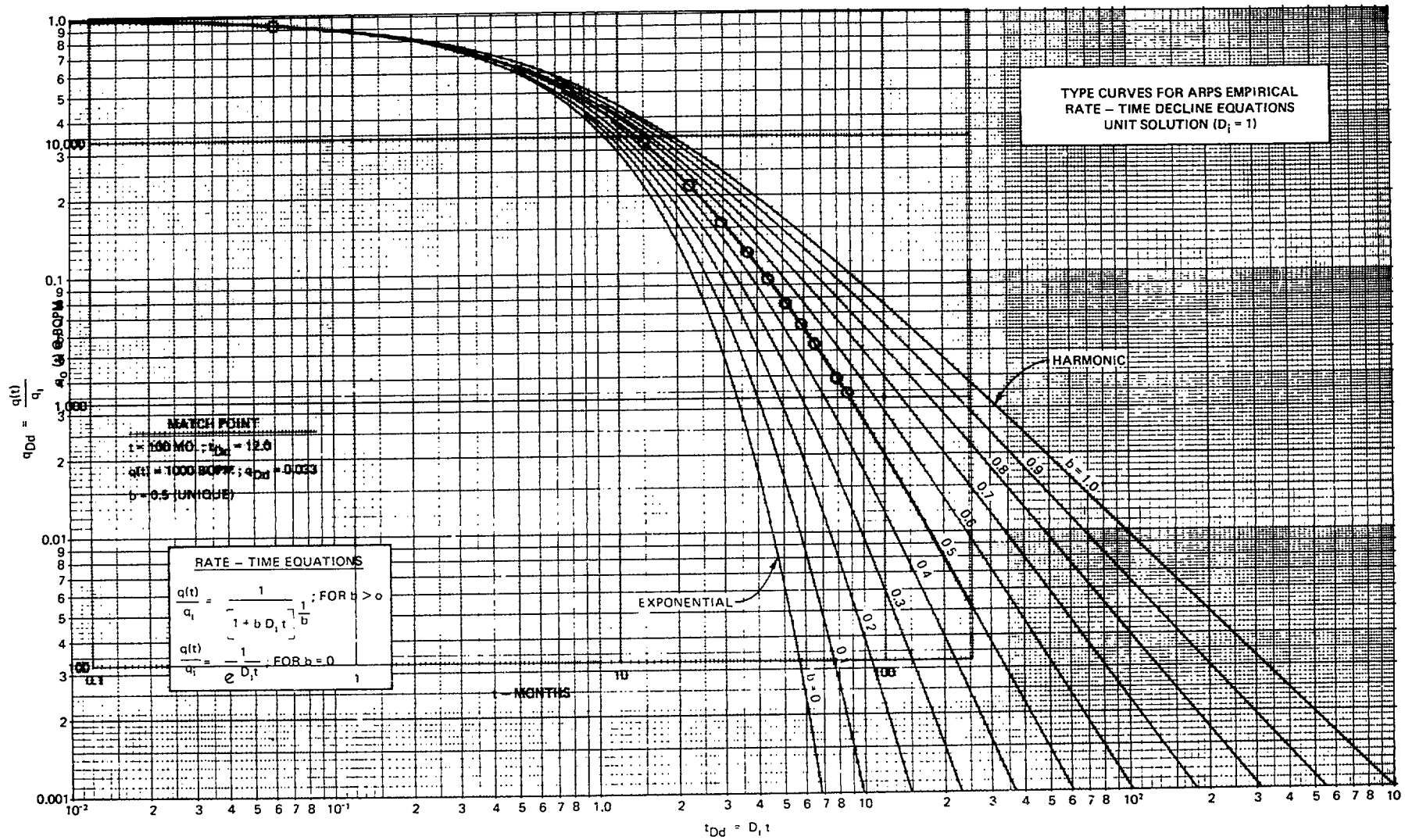


Fig. 10 - Type-curve match of Arps' hyperbolic decline example,⁴ (unique match).

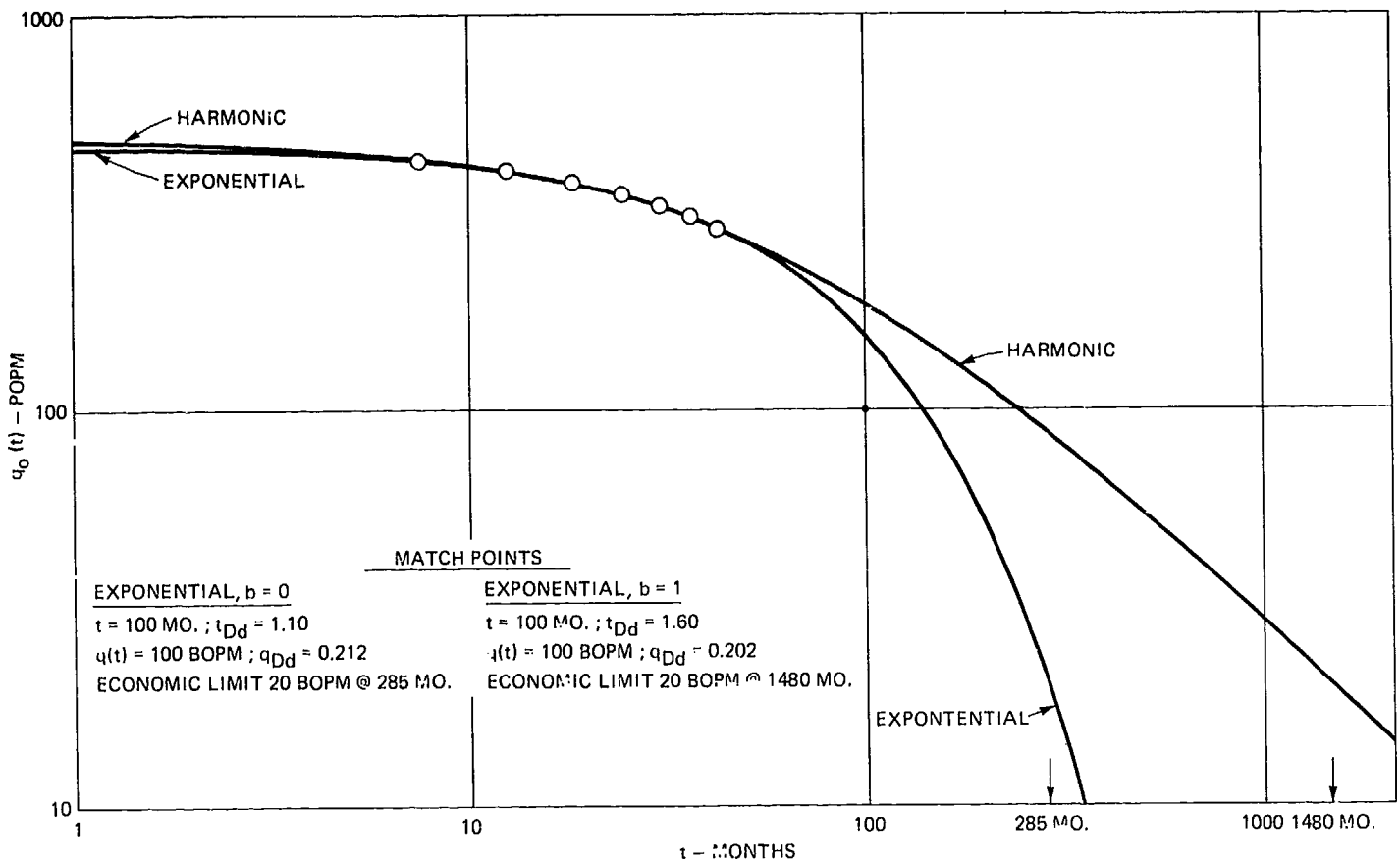


Fig. 11 - Type-curve analysis of Arps' exponential decline example.

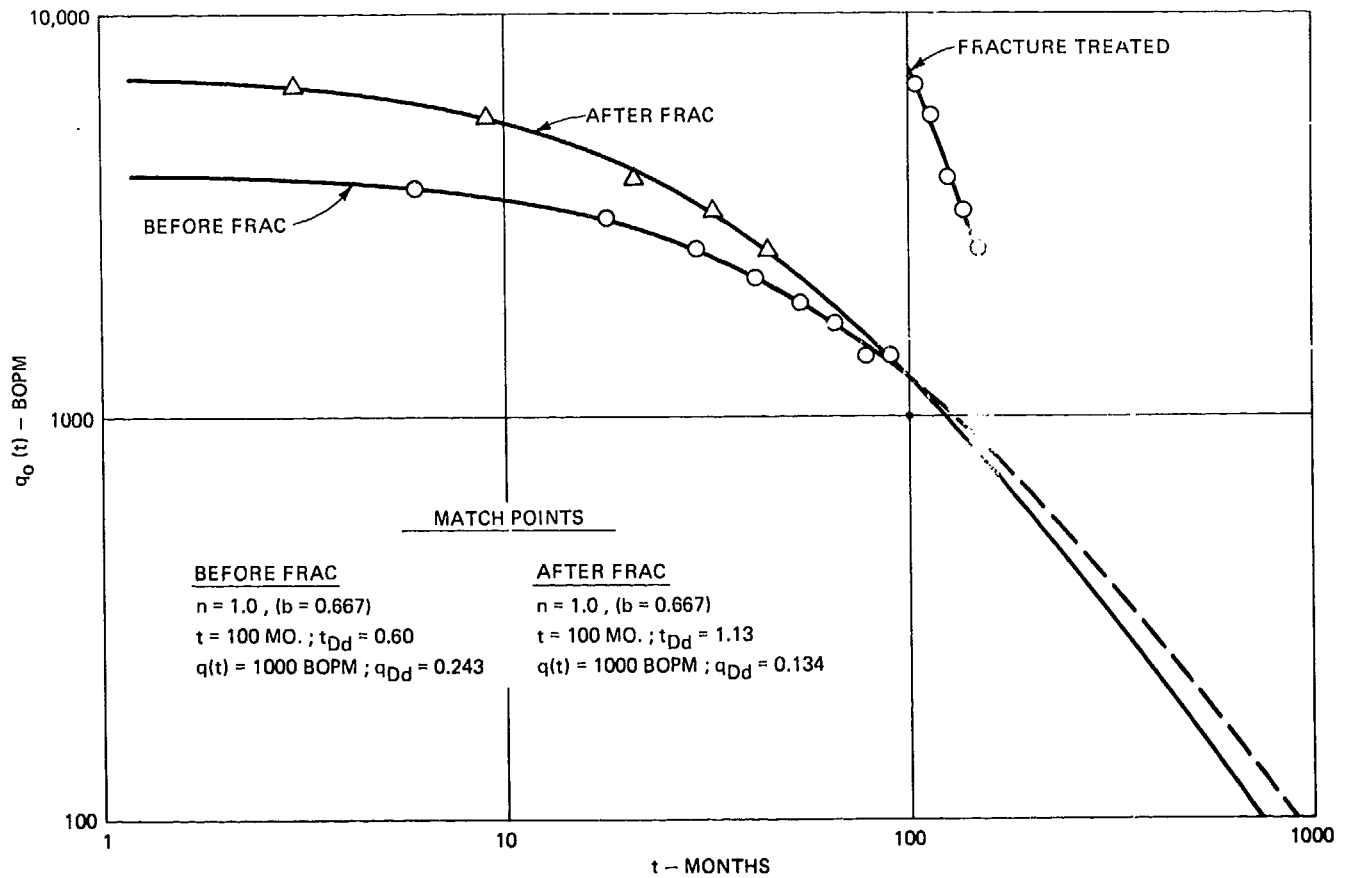


Fig. 12 - Type-curve analysis of a stimulated well before and after fracture treatment.

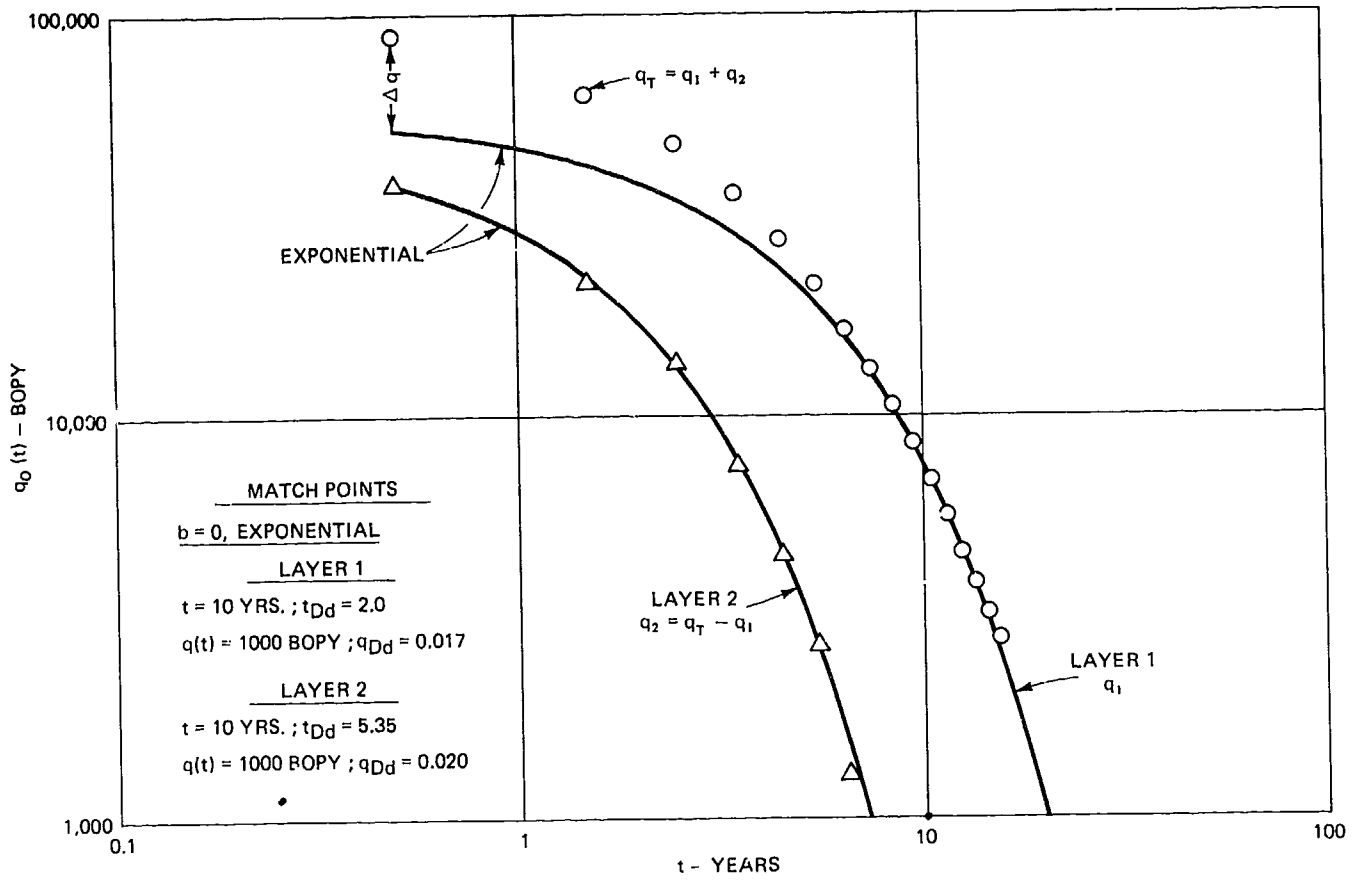


Fig. 13 - Type-curve analysis of a layered reservoir (no crossflow) by differencing.

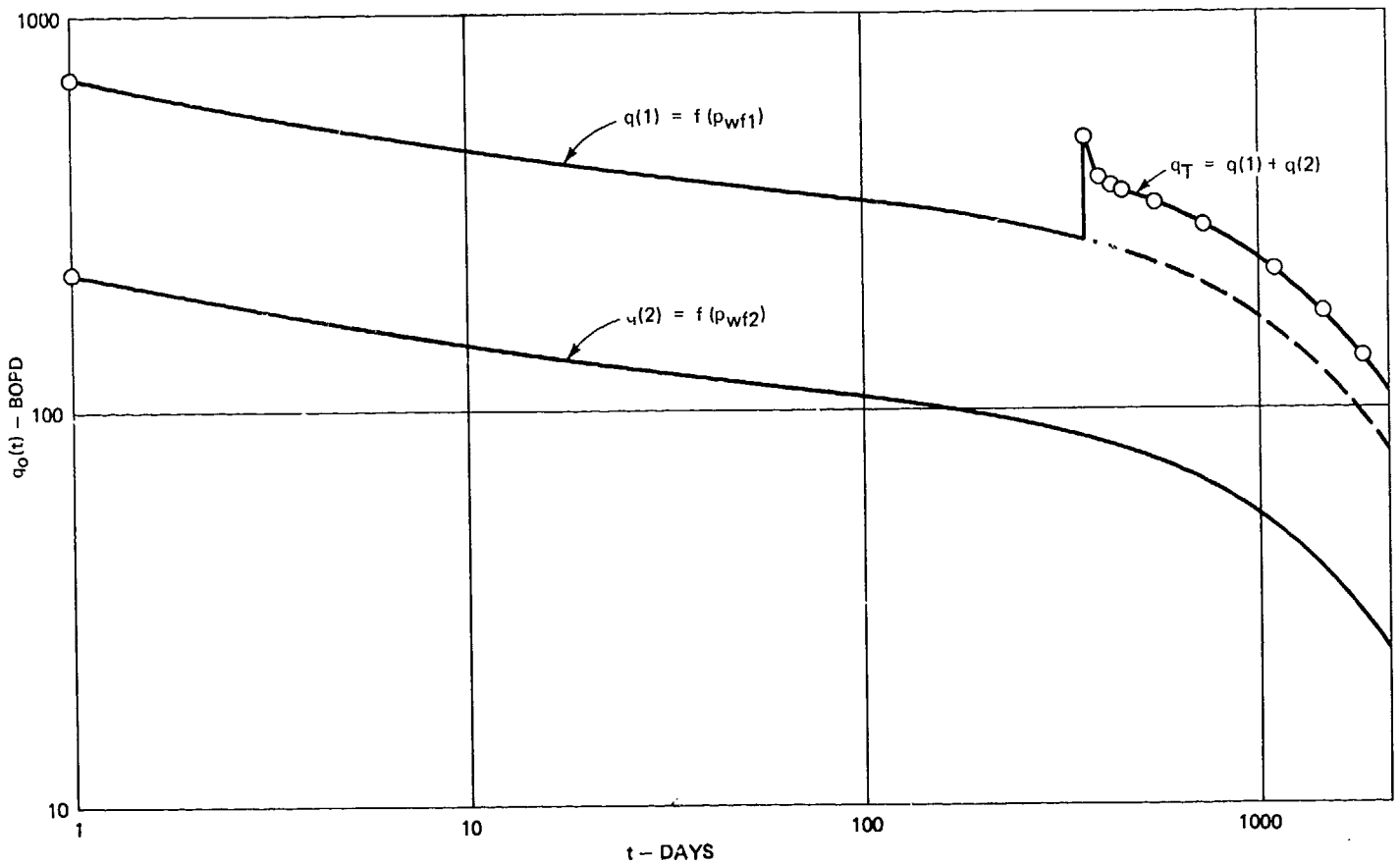


Fig. 14 - Effect of a change in back pressure on decline using graphical superposition.

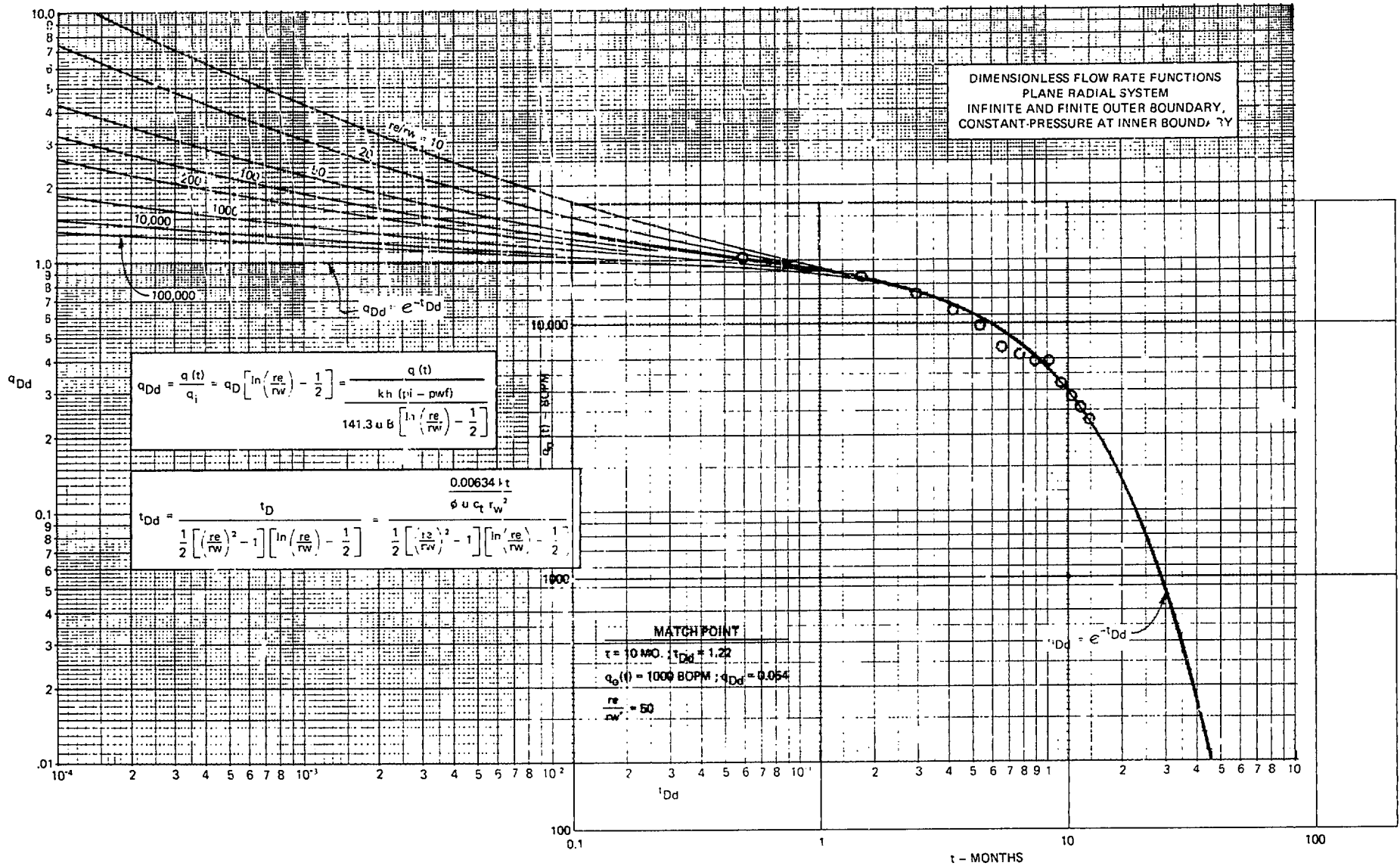


Fig. 15 - Type-curve matching example for calculating Kh using decline curve data, Well 13, Field A.

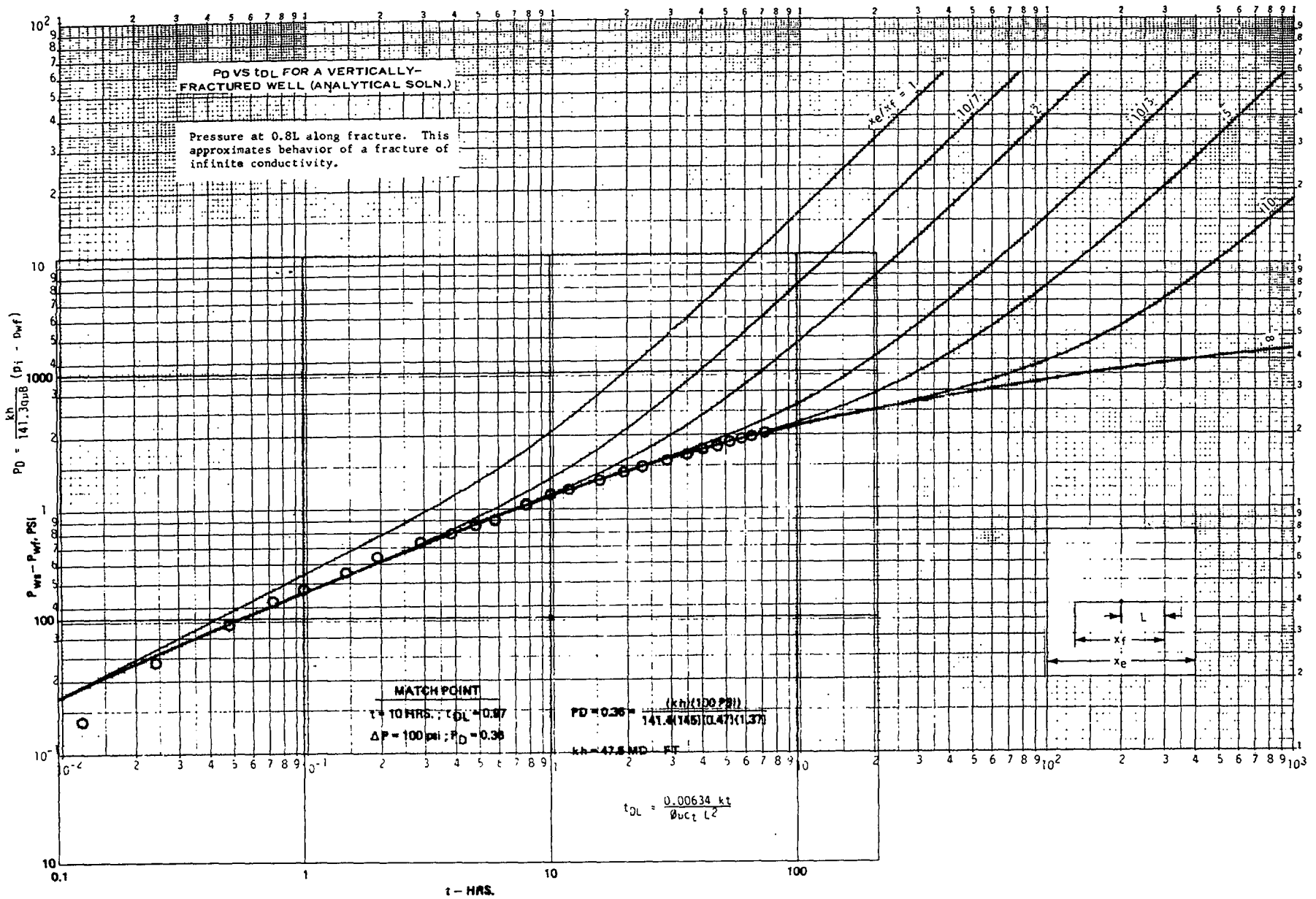


Fig. 16 - Type-curve matching example for calculating Kh from pressure buildup data, Well 13, Field A (type curve from Ref. 8).